

THE ROLE OF SIM2S IN CELL CYCLE REGULATION AND DNA DAMAGE
RESPONSE

A Thesis

by

LAUREN M. SCHILLING

Submitted to the Office of Graduate Studies of
Texas A&M University
in partial fulfillment of the requirements for the degree of

MASTER OF SCIENCE

December 2010

Major Subject: Genetics

The Role of Sim2s in Cell Cycle Regulation and DNA Damage Response

Copyright 2010 Lauren M. Schilling

THE ROLE OF SIM2S IN CELL CYCLE REGULATION AND DNA DAMAGE
RESPONSE

A Thesis

by

LAUREN M. SCHILLING

Submitted to the Office of Graduate Studies of
Texas A&M University
in partial fulfillment of the requirements for the degree of

MASTER OF SCIENCE

Approved by:

Chair of Committee,	Weston Porter
Committee Members,	Stephen Safe
	Thomas Spencer
	Charles Long

Intercollegiate Faculty Chair,	Craig Coates
-----------------------------------	--------------

December 2010

Major Subject: Genetics

ABSTRACT

The Role of Sim2s in Cell Cycle Regulation and DNA Damage Response. (December 2010)

Lauren M. Schilling, B.S., Texas A&M University

Chair of Advisory Committee: Dr. Weston Porter

Single-minded-2s (Sim2s) is a member of the basic helix-loop-helix Per-Arnt-Sim (bHLH-PAS) family of transcription factors. Members of this family play important roles in sensing and responding to environmental changes, controlling circadian rhythms, and development. Previous work in our laboratory found that Sim2s is down-regulated in human breast cancer patients and cell lines and over-expression of Sim2s in highly invasive breast cancer cells blocks their proliferative and invasive potentials. Additionally, when Sim2s is knocked-down in MCF7 breast cancer cells, this normally relatively non-aggressive cell line becomes highly invasive and metastatic.

In the studies presented here, we found that over-expression of Sim2s in MCF7 cells caused these cells to have a significant decrease in proliferative ability. Propidium iodide flow cytometry showed more Sim2s cells in the G2/M and S phases of the cell cycle as compared to Empty controls. While we observed no changes in cyclin or CDK levels between Empty controls and Sim2s cells, the regulatory protein p21 was found to be significantly up-regulated in Sim2s cells at both the RNA and protein levels. Additionally, we confirmed a cellular senescence phenotype in the Sim2s cells through

markers such as β -galactosidase staining, and Western blot analysis of Ki67 and H3K9Me2. Based on these results, we hypothesize that over-expression of Sim2s triggers an up-regulation of p21, resulting in cellular senescence and cell cycle arrest. We also found that Sim2s cells are more highly sensitized to DNA damage through clonogenic survival assays. Together, these studies support the idea that Sim2s is involved in cell cycle control by up-regulation of p21 resulting in cellular senescence and the DNA damage response by sensitizing cells to genotoxic reagents.

DEDICATION

This work is dedicated to my family. Thank you for your constant love and support—and for always believing in me.

ACKNOWLEDGEMENTS

I would like to acknowledge my advisor, Dr. Weston Porter, for giving me the opportunity to explore all aspects of graduate school and giving me the freedom to actively pursue my interests. I would also like to thank my committee members, Dr. Stephen Safe, Dr. Thomas Spencer, and especially Dr. Charles Long, for their help and advice. I have to thank the past and present members of the Porter laboratory—without them life would have been a lot less interesting and a lot more difficult. I want to thank Dr. Roger Smith for his help with all of the flow cytometry. Finally, thank you to all of the people in the Genetics, Toxicology and VIBS departments who helped me so often and made my life easier.

NOMENCLATURE

ARNT	Aryl Hydrocarbon Receptor Nuclear Translocator
ATM	Ataxia Telangectasia, mutated
ATR	ATM and RAD3 related
bHLH	basic Helix- loop-Helix
CDK	Cyclin Dependent Kinase
CDKN1a	Cyclin Dependent Kinase Inhibitor 1a (p21)
ChIP	Chromatin Immunoprecipitation
CNS	Central Nervous System
DSB	Double stranded break
ECM	Extraceellular Matrix
IR	Irradiation
MMTV	Mouse mammary tumor virus
PAS	Per-Arnt-Sim
PCNA	Proliferating Cell Nuclear Antigen
Q-PCR	Quantitative PCR
RT-PCR	Reverse Transcriptase PCR
Sim2s	Singleminded-2 short
UV	Ultraviolet
WT	Wild-type

TABLE OF CONTENTS

	Page
ABSTRACT	iii
DEDICATION	v
ACKNOWLEDGEMENTS	vi
NOMENCLATURE	vii
TABLE OF CONTENTS	viii
LIST OF FIGURES	x
LIST OF TABLES	xii
CHAPTER	
I INTRODUCTION: CANCER, CELL CYCLE, p21-INDUCED SENESCENCE	1
Overview of Cancer and Sim2s	1
Cell Cycle Regulation	9
Cellular Response to DNA Damage	11
Cellular Senescence	14
Mechanism of Oncogene-Induced Senescence	16
Role of p21 in Cellular Senescence	17
II MATERIALS AND METHODS	22
Cell Culture	22
Lentiviral Transduction	22
PCR Analysis	24
Chromatin Immunoprecipitation Assay (ChIP)	26
Western Blot Assay	28
β -Galactosidase Staining	30
Clonogenic Survival Assay	30
Proliferation Assay	32
Flow Cytometry	33
DIC Imaging	34

CHAPTER	Page
Statistical Analysis	34
III THE ROLE OF SIM2S IN CELL CYCLE REGULATION	35
IV THE ROLE OF SIM2S IN DNA DAMAGE RESPONSE AND CELLULAR SENESENCE.....	40
V CONCLUSIONS	50
REFERENCES	58
VITA.....	64

LIST OF FIGURES

FIGURE	Page
1 Cancer incidences for individuals with Down syndrome	5
2 Expression levels of Sim2s were surveyed in a panel of human breast cell lines	7
3 Proliferation assay for MDA-MB-435 cells over-expressing Sim2s and Empty controls	7
4 Analysis of invasive potential and ECM markers in MCF7 cells with Sim2s knocked down.....	8
5 Graphical representation of the cell cycle	9
6 DNA damaging reagents incite cellular response by activating ATM or ATR.....	15
7 Overview of cellular response to oncogenic stress.....	19
8 Cyclin dependent kinase inhibitor p21 can effect cell cycle arrest at all stages of the cell cycle	20
9 pLPCX vector map	23
10 Proliferation assay on MCF7 pLPCX-Empty and Sim2s cells	36
11 Propidium iodide flow cytometry of MCF7 pLPCX-Empty and Sim2s cells.....	37
12 Western blot analysis of major cyclins and CDKs involved in cell cycle..	38
13 Real Time PCR assay of expression levels of regulatory protein RNA levels and Western blot analysis of GADD45	39
14 Real Time PCR assay and Western blot analysis of p21	41
15 Over-expression of Sim2s regulates p21 expression in response to DNA damage.....	42

FIGURE		Page
16	Clonogenic survival assay of MCF7 pLPCX-Empty and Sim2s cells to ascertain survival upon exposure to genotoxic stress.....	44
17	ChIP analysis of MCF7 pLPCX-Empty and Sim2s cells upon exposure to UV radiation.....	45
18	DIC images of Sim2s over-expressing MCF7 cells and Empty controls...	47
19	MCF7 pLPCX-Sim2s cells have increased β -galactosidase staining as compared to Empty controls.....	48
20	Western blot analysis of cell proliferation marker Ki67 and apoptotic marker PARP.....	49
21	Proposed role of Sim2s in cell cycle arrest and cellular senescence	57

LIST OF TABLES

TABLE		Page
1	Primer sequences for all Real Time PCR reactions.....	25
2	Conditions and sequences for ChIP PCR primers	28
3	Conditions for antibodies used	31

CHAPTER I

INTRODUCTION: CANCER, CELL CYCLE, p21-INDUCED SENESCENCE

Overview of Cancer and Sim2s

Cancer is the second most common cause of death in the United States, exceeded only by heart disease. In 2009 alone 562,340 Americans were expected to die of cancer—nearly 1 of every 4 deaths (1).

Breast cancer is the second leading cause of cancer-related deaths in U.S. women and the fourth leading cause of death in women overall. In 2009, over 40,000 women died from this disease and 192,370 new cases were diagnosed. While survival rates for women with breast cancer have been slowly increasing over the years due to better/early detection and improved treatment methods, it is important to further increase survival rates by developing better forms of treatment and ultimately preventative measures. For this reason, research on breast cancer is extremely important. The objective of our research with Single-minded2-s (Sim2s) is to ultimately contribute to this research and establish additional and improved forms of detection or treatment for breast cancer. Before we can reach that step, however, we need to establish how Sim2s functions in the breast and its role in cell cycle regulation and DNA damage response.

This thesis follows the style of Cancer Research.

Single-minded2-s (*Sim2s*) is a member of the basic helix-loop-helix Per-Arnt-Sim (bHLH/PAS) family of transcription factors. This family includes members such as Per, Hif1 α , and ARNT; factors involved in circadian rhythm, response to environmental stressors (hypoxia), and regulation of transcriptional responses to dioxins and polycyclic aryl hydrocarbons. The PAS domain is highly conserved and has many important roles in sensing and binding to small molecules such as molecular oxygen, cellular metabolites, or polyaromatic hydrocarbons (2).

Many PAS family members play important roles in regulating development. In *Drosophila*, Single-minded (Sim) is required for synchronized cell division, proper formation of nerve cell precursors, and positive auto-regulation of central midline expression—thus making it a master developmental regulator of the CNS (3-4). In mammals there are two different Sim homologs (Sim1 and Sim2). Null mutations in both genes in mice have provided evidence that both genes are important for embryonic survival as both Sim1 and Sim2 knock-out mice die shortly after birth (5). Work in mice has shown that Sim1 is required for development of several secretory neurons at the final stages of their differentiations (6). Mice that have had Sim2 knocked-out die within 3 days of birth due to lung atelectasis and breathing failure. Additionally, these mice have congenital scoliosis, as observed in the unequal sizes of the left and right vertebrae and ribs. The temporal and spatial expression patterns of Sim2 indicate that it could play a role in regulating skeletal growth and/or development (7).

The Sim2 gene has a splice variant referred to as Sim2s. This variant is missing part of exon 11, which contains a carboxyl Pro/Ala-rich repressive domain. Both Sim2

and Sim2s repress Dioxin Response Elements (DREs) equally, however, they have differential responses in repressing Hypoxia Response Elements (HREs), with Sim2s having a less repressive effect. Additionally, Sim2s can activate expression from a Central Midline Element (CME). This implies that the Pro/Ala-rich sequence present in Sim2 but not Sim2s exerts a negative effect on CME-mediated gene expression (8).

Our laboratory has previously shown that Sim2s is developmentally regulated in the mammary glands of mice and its expression peaks during the first week of lactation when the mammary gland is undergoing terminal differentiation. Precocious expression of Sim2s *in vivo* promotes an alveolar cell phenotype. Analysis of mammary glands from transgenic mice over-expressing Sim2s under the Mouse Mammary Tumor Virus (MMTV-Sim2s) and wild-type (WT) mice found that mRNA levels of milk proteins including β -casein (Csn2) and whey acidic protein (WAP) were significantly increased in the mice over-expressing Sim2s (9-10). Further, we hypothesized that Sim2s is involved in enhanced mammary gland differentiation because we observed an increase in the sodium phosphate transporter Npt2b (shown to be expressed in late pregnant and lactating mammary tissues) in transgenic mice (9-10).

The Sim2 gene is found on Chromosome 21 (in humans) and 16 in mice (syntenic to Human Chromosome 21). Transgenic mice with three copies of Sim2 exhibit a slight Down Syndrome phenotype (11). Additionally, these mice die at birth from complications due to breathing failure and display rib, vertebral and craniofacial abnormalities (7).

Due to its location on Chromosome 21 in the Down Syndrome Critical Region, Sim2s plays an important role in the etiology of this disorder. Sim2 mRNA is expressed in facial, skull, palate and vertebra primordia in human and rodent embryos and its trisomic state is suspected to contribute to the phenotypic features associated with Down Syndrome (DS), as well as, the anxiety-related/reduced exploratory behavior and sensitivity to pain phenotypes of DS individuals (11-12). Like many genetic disorders, DS has a unique tumor profile. These individuals have an increased incidence of leukemia and ovarian or testicular cancer, but a decreased incidence of solid tumors—in particular breast cancer (Figure 1). In several age-matched control studies, individuals with DS were shown to have a significantly decreased incidence of breast cancer (13-14).

Because of this dramatically decreased incidence of breast cancer in these individuals, our laboratory is investigating the potential role of Sim2s as a tumor suppressor gene in the breast. While Sim2s is shown to be up-regulated in prostate and pancreatic cancers, the supposed oncogenic mechanism has not been delineated, and like several genes such as KLF4, Sim2s could play a role as an oncogene in one tissue and a tumor suppressor in another (4, 16).

Site (ICD-7)	Observed	Expected	SIR (95% CI)
All sites (140–205)	60	49.83	1.20 (0.92–1.55)
Buccal cavity (140–148)	0	1.04	0.00 (0.0–2.88)
Digestive system (150–159)	4	6.52	0.61 (0.17–1.57)
Stomach (151)	1	0.91	1.10 (0.01–6.14)
Colon (153)	2	2.24	0.89 (0.10–3.23)
Peritoneum (158–159)	1	0.01	67.77 (0.89–377)
Respiratory system (160–164)	1	4.96	0.20 (0–1.12)
Lung (162)	1	4.22	0.24 (0–1.32)
Breast (170)	0	7.32	0.00 (0.0–0.41)
Female genital organs (171–176)	4	5.68	0.70 (0.19–1.80)
Uterus (172)	1	1.20	0.83 (0.01–4.63)
Ovary (175)	3	1.52	1.97 (0.40–5.77)
Male genital organs (177–179)	4	2.82	1.42 (0.38–3.63)
Testis (178)	4	2.15	1.86 (0.50–4.77)
Urinary tract (180–181)	4	2.97	1.35 (0.36–3.45)
Kidney (180)	1	1.19	0.84 (0.01–4.66)
Bladder (181)	3	1.78	1.69 (0.34–4.93)
Skin (190–191)	2	8.14	0.25 (0.03–0.89)
Non-melanoma	2	5.76	0.35 (0.04–1.25)
Other specified sites (192–197)	2	4.75	0.42 (0.05–1.52)
Eye (192)	1	0.27	3.68 (0.05–20.5)
Brain (193)	1	3.32	0.30 (0–1.68)
Secondary and unspecified sites (198–199)	3	0.92	3.27 (0.66–9.56)
Non-Hodgkin lymphoma (200, 202)	0	1.41	0.00 (0.0–2.13)
Hodgkin's disease (201)	0	0.92	0.00 (0.0–3.25)
All solid tumours (140–202)	24	47.77	0.50 (0.32–0.75)
Leukaemia (204)	36	2.04	17.63 (12.4–24.4)
ALL	20	0.82	24.36 (14.9–37.6)
AML	12	0.59	20.28 (10.5–35.4)
Acute unspecified leukaemia	3	0.11	26.86 (5.4–78.5)
Leukaemia not otherwise specified	1	0.52	1.93 (0.03–10.8)

Figure 1. Cancer incidences for individuals with Down syndrome. Adapted from (15).

Initially we surveyed Sim2s expression in a variety of human breast cell lines. Interestingly, Sim2s levels were high in normal breast cells but severely decreased in breast cancer lines (Figure 2) (17). Additionally, as the invasive potential of the breast cancer cell lines increased, Sim2s levels decreased. To investigate the potential tumor suppressor activity, we over-expressed Sim2s in highly invasive MDA-MB-435 cells, which resulted in inhibited proliferation and invasive potential (Figure 3).

Additionally, knock-down of Sim2s in the relatively non-invasive MCF7 breast cancer cell line resulted in an epithelial-mesenchymal transition (EMT) characterized by a spindled cell morphology with decreased epithelial characteristics and significantly elevated mesenchymal markers (Figure 4). When control and Sim2s-deficient (Sim2i) MCF7 cells were injected into the flanks of nude mice, the Sim2i cells resulted in large, highly vascularized, estrogen receptor negative tumors. Together, these results support a role for Sim2s as a breast tumor suppressor.

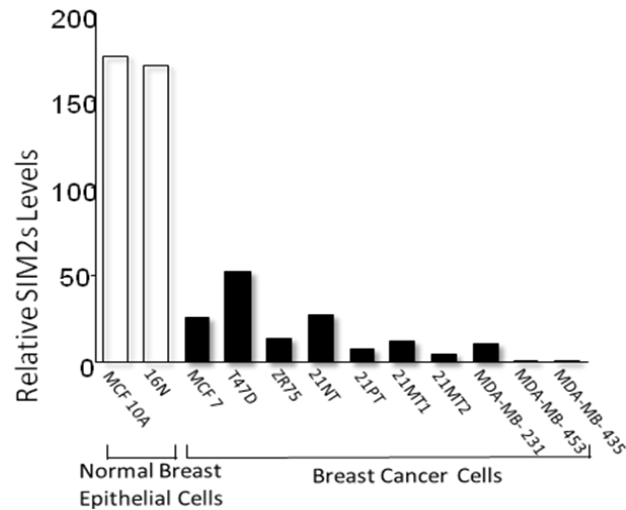


Figure 2. Expression levels of Sim2s were surveyed in a panel of human breast cell lines. Sim2s levels were highly expressed in normal breast epithelial cells but decreased in breast cancer cells, with the lowest levels found in the most highly invasive cell lines (17).

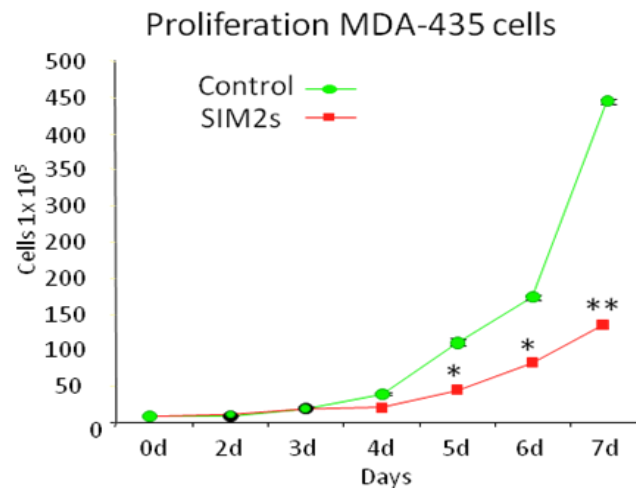


Figure 3. Proliferation assay for MDA-MB-435 cells over-expressing Sim2s and Empty controls. When Sim2s is over-expressed in the highly invasive MDA-MB-435 cell line, the proliferative ability of these cells is decreased as compared to control cells [Adapted from (17)].

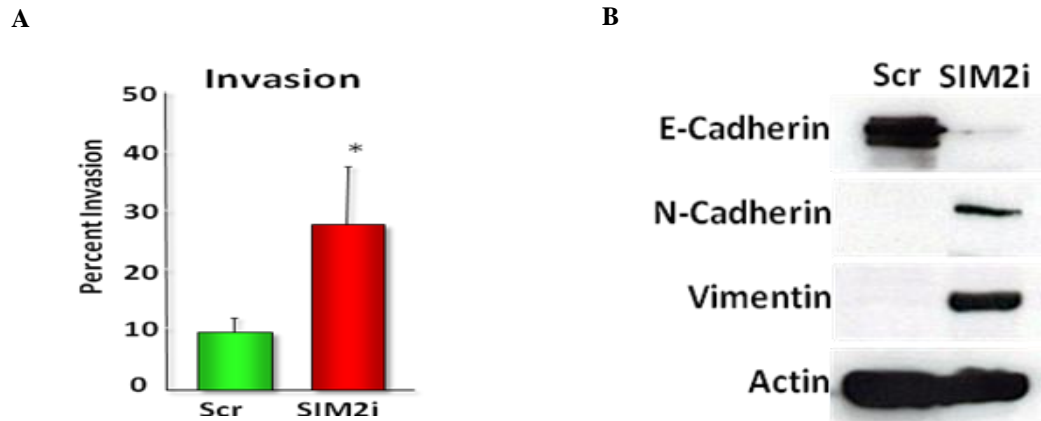


Figure 4. Analysis of invasive potential and ECM markers in MCF7 cells with Sim2s knocked down. **A.** When Sim2s is knocked-down in the less-invasive breast cancer cell line MCF7 the invasiveness potential of these cells significantly increases. **B.** Additionally, these cells appear to undergo an epithelial to mesenchymal like-transition, with epithelial markers like E-Cadherin becoming down-regulated and mesenchymal markers such as N-cadherin and vimentin increasing (18).

Cell Cycle Regulation

Throughout the course of the cell cycle, mammalian cells coordinate several different physiological processes, including: coordinating cell growth, genome replication, and cellular division. There are four major parts of the cell cycle—G1, S, G2, and M, and each are regulated by a variety of signaling molecules and other proteins, including cyclins and cyclin dependent kinases (Figure 5).

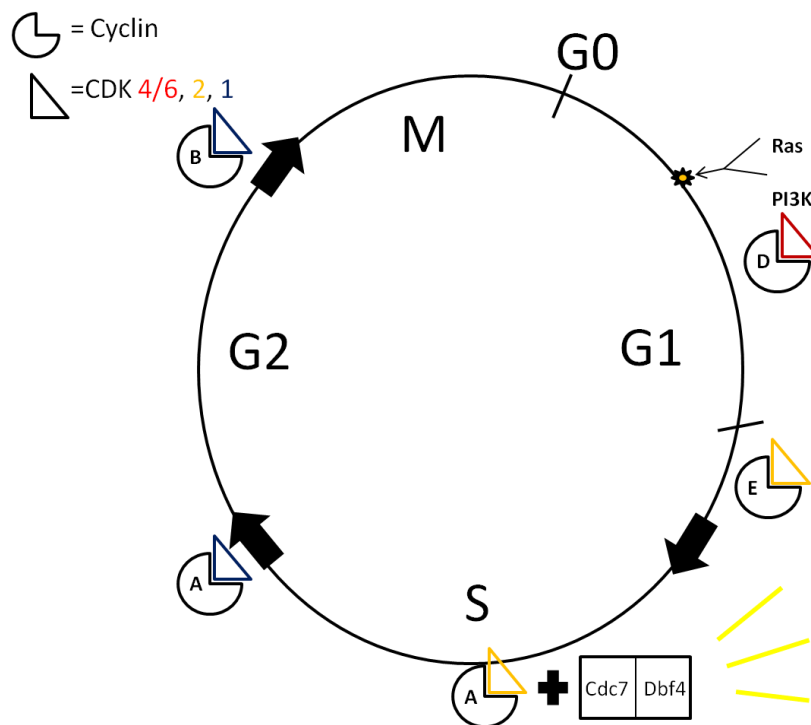


Figure 5. Graphical representation of the cell cycle. Major cyclins and CDKs are shown, as well as some of the major factors required to push the cell through the various phases of the cell cycle. Hyperphosphorylated Retinoblastoma is required to push the cell through the R-point (where it is no longer responsive to mitogenic signaling) and into S-phase.

Before a cell can begin to replicate its DNA in S-phase, it “consults” its extracellular environment and responds to growth stimulating signals. It is of particular note that cells are only susceptible to mitogenic signaling during the G1 phase. Mitogenic signaling through receptor tyrosine kinases and G-protein coupled receptors activate pathways such as Ras and PI3K to stimulate cell proliferation, growth, and survival—pushing the cell through G1. The Ras-MEK-ERK kinase cascade promotes activation of CDK2 by ERK-dependent phosphorylation and stabilization of c-Myc. This, in turn, induces expression of cyclin D1 and suppresses CDK inhibitors (19). The PI3K pathway is important for G1 because it activates Akt which inhibits glycogen synthase kinase 3- β (GSK3- β) and prevents it from destabilizing cyclin D. The D-family of cyclins (D1, 2 and 3) is involved in regulating G1. At the beginning of G1, a D-cyclin pairs with CDK4 or 6 (two very similar CDKs). However, as Retinoblastoma (Rb) becomes more highly phosphorylated and drives the cell through the Restriction-point (R-point) CDK4 and 6 are replaced with CDK2, and cyclin D is replaced by cyclin E. After the cell passes through the R-point, it is no longer responsive to mitogenic signaling.

In the beginning of S-phase, cyclin A replaces cyclin E and partners with CDK2. These complexes concentrate at the replication foci on chromosomes. Initiation of DNA synthesis at replication origins is triggered by S-Cdks and Cdc7, an additional protein kinase. Cdc7 activity is activated by binding to a regulatory subunit, Dbp4. These protein kinases enable pre-replicative complexes (PRCs) to recruit DNA helicases, primases and polymerases (19). In addition, they enable the PCNA complex to close

around the DNA template strand and move freely along it, thus beginning DNA replication. As S-phase continues, cyclin A dissociates from CDK2 and partners with CDK1 (also known as CDC2).

Before the cell can enter mitosis and divide into two cells, it passes through a second gap phase, G₂. During this phase the cell prepares itself for entry into mitosis. Starting in S-phase, transcription of cyclin B is up-regulated and while initially, in G₂, cyclin A is bound to CDC2, as the cell moves further through this phase, cyclin A is replaced by cyclin B as it moves from the cytoplasm into the nucleus. When cyclin B binds to CDC2 the complex is not activated until CDC2 is phosphorylated on T161 by Cdk-activating kinase (CAK). CDC2 in complex with cyclin B remains active until late interphase of mitosis. At this point, CDC2 is phosphorylated at T14 and Y15 which results in an inhibition of its kinase activity. This phosphorylation activity is controlled by Wee1 and Myt1 kinases and Cdc25 phosphatases (20).

After cells have gone through G₂, they enter mitosis—which is composed of several different phases: prophase, metaphase, anaphase and telophase. An extremely complex array of proteins and other molecules regulate the cells transition through these steps. After the cells have undergone mitosis, one parental cell results in two new daughter cells.

Cellular Response to DNA Damage

At each of the individual phases of the cell cycle there is a checkpoint to prevent the replication of the cell if it has been exposed to DNA damage. While there are many

factors involved in different pathways that can arrest cells at various checkpoints, only a few major ones will be discussed in this section. The G1 checkpoint prevents damaged DNA from being replicated, while the S-phase checkpoint functions to monitor cell cycle progression and to react to DNA damage by decreasing synthesis. The G2 checkpoint is the final checkpoint that can prevent a cell with damaged DNA from replicating by suspending the cell cycle before chromosomes segregate. There are two key regulators of the DNA damage pathway, Ataxia telangectasia, mutated (ATM) and ATM and Rad3 related (ATR) protein kinases. These regulators affect cell cycle arrest at all three of the cell cycle checkpoints. Usually, ATM is the primary response when a cell undergoes a DNA double strand break (DSB) upon exposure to ionizing radiation (IR). ATR plays the main role in reacting to DSBs caused by UV damage and stalls in DNA replication, but also plays a back-up role when cells are exposed to IR.

The G1 checkpoint is controlled by the ATM/ATR kinases which control the actions of p53. When cells are exposed to ionizing radiation (IR), ATM phosphorylates T68 of Chk2 which then phosphorylates S20 of p53. Phosphorylated S20 in p53 inhibits its interaction with MDM2, preventing p53 from being ubiquitinated (21). ATM can also directly inhibit MDM2 by phosphorylating it at S395, preventing its interaction with p53. When p53 is up-regulated at the G1 checkpoint, it results in the activation of p21—a cyclin-dependent kinase inhibitor which suppresses the kinase activity of cyclin E/cdk2 and causes the cell to arrest in G1 (22).

The S checkpoint is the least well understood of the three. Some experiments have shown that in mammalian cells ATR is responsible for activating Chk1 (although it

has also been shown to activate Chk2). This leads to hyperphosphorylation of Cdc25A and inhibition of the CDK2/cyclin E complex. The result of this inhibition is decreased DNA replication origin firing and an activation of DNA repair pathways (23). However, other experiments have shown that IR damage can activate the S-phase checkpoint by activating ATM which then phosphorylates T68 of Chk2. This phosphorylation of Chk2 targets Cdc25A for ubiquitinylation (by phosphorylating it at S123). As the normal function of Cdc25A is to remove inhibitory phosphorylations (T14 and Y15) from Cdk2, without functional Cdc25A the CDK2/cyclin E and CDK2/cyclin A complexes are prevented from enabling DNA synthesis (24).

At the G2 checkpoint in response to IR, UV, and genotoxic reagents, ATM/ATR phosphorylate Chk1/Chk2 which then phosphorylate Cdc25C at S216 (Figure 6). When this site is phosphorylated it allows binding of 14-3-3 proteins. The 14-3-3/Cdc25C protein complexes are sequestered in the cytoplasm. This prevents Cdc25C from activating Cdc2 which inhibits Cdc2/Cyclin B1 complex formation and cell cycle progression. This causes the cells to arrest in G2. In response to damage, p53 transcriptionally up-regulates expression of GADD45 and p21. GADD45 is responsible for dissociating Cdc2 from cyclin B1 in response to damage and p21 interacts directly with Cdc2. Both of these pathways enable the cell to arrest in G2 (25). Alternatively, p21 can function independently of p53 activation—and can cause cell cycle arrest at all phases of the cell cycle.

Cellular Senescence

In 1961 Hayflick observed that diploid cells in serial culture permanently stop dividing after approximately 50 passages. These cells were irreversibly arrested and no longer able to divide despite being viable and metabolically active. This state is known as cellular senescence and is characterized by the inability of cells to proliferate despite access to abundant nutrients and mitogens (26). While there is evidence showing that cellular senescence in human cells is genetically controlled through telomere shortening, it can also be caused in response to loss of tumor suppressors or oncogene activation and acts hand-in-hand with apoptosis to limit tumorigenic expansion (27). The discovery that cellular senescence is triggered by multiple activated oncogenes has led to the idea that senescence (like oncogene-induced apoptosis) is a critical and cell autonomous tumor preventative mechanism (26). Additional evidence for cellular senescence acting as a barrier to cancer exists. Most tumors contain cells that appear to have evaded senescence. This extended replicative lifespan increases a cell's susceptibility to malignant progression because it permits cell divisions that might acquire successive mutations. Recently, it has been shown that senescence is not just a passive proliferation arrest that impacts only the senescent cell. Instead, these cells influence their environment and neighboring cells through an active secretory system—producing different growth factors that stimulate the growth of neighboring cells. For example, p21 expression in mammalian development has been localized to narrow zones of postmitotic cells which are directly adjacent to proliferative compartments (28-29).

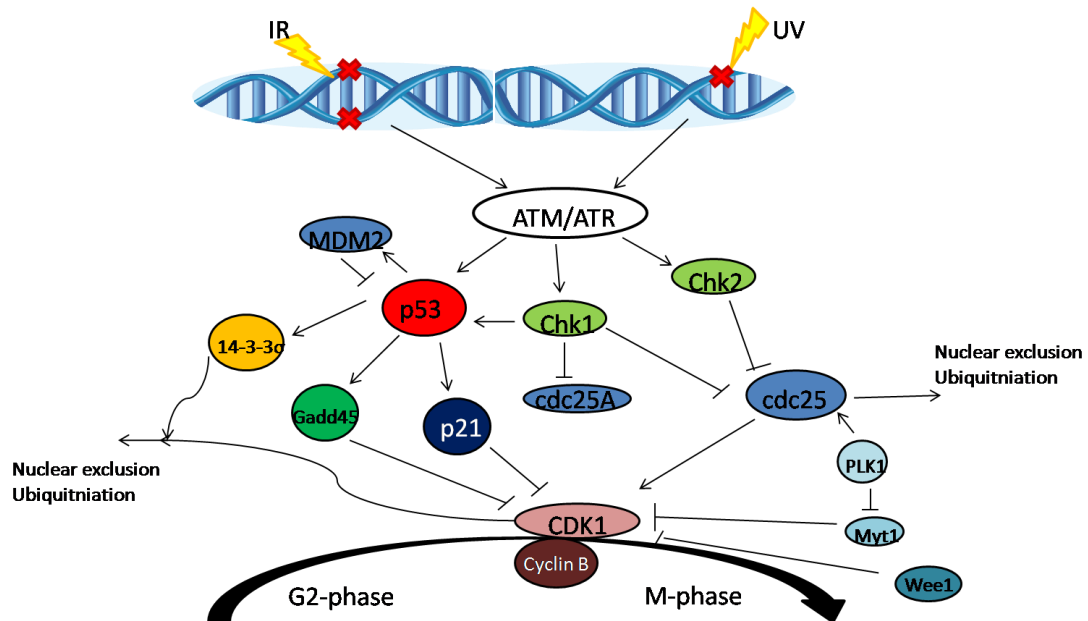


Figure 6. DNA damaging reagents incite cellular response by activating ATM or ATR. These proteins can further activate a variety of additional regulatory proteins to result in cell cycle arrest at the G2/M phase of the cell cycle. Other regulatory factors can affect arrest at the other stages of the cell cycle.

Mechanism of Oncogene-Induced Senescence

While many different oncogenes and growth regulatory molecules trigger senescence, the pathways that have been best described are for mutated oncogenic Ras and its effectors. Chronic signaling through the Ras-Raf-MEK-ERK pathway drives senescence through activation of the p38 MAP-kinase-p16 stress response pathway (28, 30). There are multiple examples of oncogenes functioning as tumor-suppressors, resulting in oncogene-induced senescence (31-34).

Oncogenic stress induces up-regulation of cyclin-dependent kinase inhibitor p16. High level expression of this protein activates Retinoblastoma (Rb), mitogenic signals, increases reactive oxygen species (ROS) and elicits a positive feedback of the ROS-PKC σ signaling pathway (35). In human somatic cells, once Rb is fully engaged, senescent cell cycle arrest becomes irreversible and cannot be revoked by subsequent inactivation of Rb and p53. Interestingly, when Rb and p53 are inactivated, senescent cells reinitiate DNA synthesis, but they subsequently fail to complete the cell cycle, suggesting that these cells arrest in G2 or M phase (35).

Additional evidence has shown that senescent cells acquire a specific gene expression profile or signature that includes the up-regulation of inflammatory cytokines. This leads to the activation of the innate immune system which can clear a tumor, establishing a link between cellular senescence and tumor suppression (27).

Role of p21 in Cellular Senescence

When cells undergo DNA damage, this is accompanied by activation of p53. Additionally, the cyclin dependent kinase inhibitor CDKN1a (p21) can be activated in both a p53-dependent and –independent manner. Induction of p21 is a common mechanism of growth arrest in cells under different physiological situations. It is transiently induced in the course of replicative senescence, reversible and irreversible forms of damage-induced growth arrest, and in terminal differentiation of post-mitotic cells (11). Within 14 hours after p21 induction, cessation of DNA replication and mitosis occurs—resulting in cells arresting not only in G1, but also in S and/or G2 phase. As Chang et al. showed, p21-9 cells (p21 is rapidly induced in these cells by addition of 50 μ M IPTG) showed morphological and senescence-associated β -galactosidase activity. This over-expression of p21 resulted in approximately equal numbers of cells arresting in G1 and G2 of the cell cycle through its interaction with and inhibition of CDKs. Additionally, p21 interaction with other genes can result in cell cycle arrest. For example, p21 binds to c-Jun amino-terminal kinases and Gadd45 resulting in a p53-independent G2 cell cycle arrest (36).

The effects of p21 on cellular gene expression was investigated using cDNA arrays determining up- and down-regulated genes associated with over-expression of p21 in p21-9 cells. Forty-three of the 69 down-regulated genes identified in the cDNA array were associated with cell cycle progression and DNA repair. This indicated that the p21-mediated inhibition of gene expression and resulting senescence is highly selective in nature. Twenty of 48 genes up-regulated by p21 encode for extracellular

matrix (ECM) components, ECM receptors and other secreted proteins. Over-expression of ECM proteins, including the p21-induced gene products fibronectin-1, plasminogen activator inhibitor 1 (PAI-I), tissue-type plasminogen activator (t-PA), and integrin β -3 are hallmarks of replicative senescence in normal fibroblasts (11).

The reason p21 can induce cell cycle arrest (and ultimately senescence) at most stages of the cell cycle is due to its ability to operate in many different pathways (Figure 7). For example, induction of p21 in G1 results in inhibition of Cdk2, and an overall inhibition of the Cdk2/Cyclin E complex. This inhibits phosphorylation of Retinoblastoma and cell cycle progression is halted. Additionally, up-regulation of p21 results in activation of p16, another cyclin dependent kinase inhibitor. Activation of p16 causes many cells to senesce in G1 phase of the cell cycle. When cells are in S-phase and p21 is induced, the kinase activities of Cdk1 and Cdk2 are inhibited and this blocks the actions of the Cdk/Cyclin A complex. These inhibitory effects result in cell cycle arrest and initiation of senescence in the S-phase of the cell cycle. Finally, in G2 p21 can either directly interact with Cdk1 to prevent Cdk1/Cyclin B from pushing the cell into mitosis, or it can interact with a variety of cell cycle regulatory proteins including 14-3-3 σ and Gadd45. These regulatory proteins can also prevent the cell from moving into mitosis permanently and this can also result in cellular senescence (Figure 8).

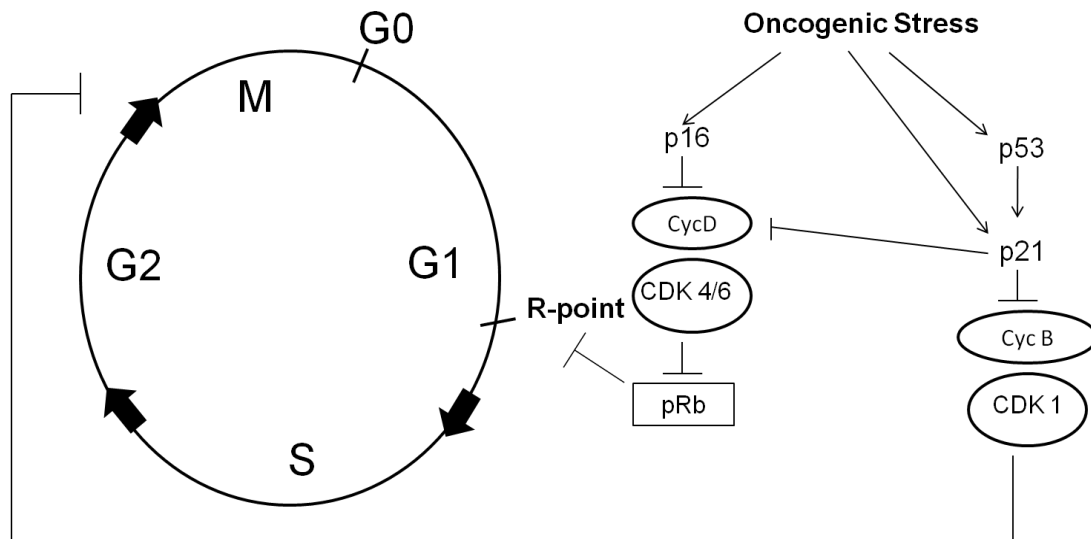


Figure 7. Overview of cellular response to oncogenic stress. This form of stress results in activation and up-regulation of p16, p53, and/or p21. These proteins activate several different pathways that ultimately result in cell cycle arrest and senescence.

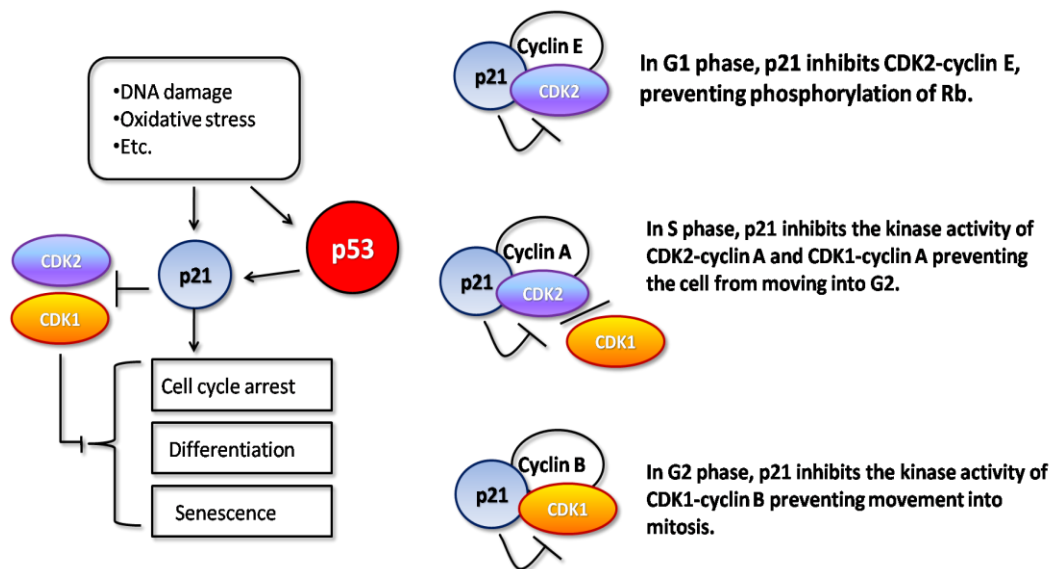


Figure 8. Cyclin dependent kinase inhibitor p21 can effect cell cycle arrest at all stages of the cell cycle. In G1 phase, p21 prevents phosphorylation of Rb, resulting in cell cycle arrest. In S-phase, p21 can inhibit the kinase activity of cdk1 and cdk2 which prevents the cell from moving into G2 phase. Similarly, in G2 phase p21 inhibits the kinase activity of cdk1 which prevents movement of the cell into mitosis.

We have shown that Sim2s is down-regulated in human breast-cancer patients and breast cancer cell lines. Re-establishment of Sim2s in highly invasive breast cancer cells results in loss of aggressive growth and metastasis. Alternately, down-regulation of Sim2s in normal immortalized breast and non-invasive breast cancer cells results in an EMT and increased invasive potential. Although these results suggest that Sim2s has breast tumor suppressor activity, the impact of Sim2s on cell cycle regulation has not been determined. The studies here, we analyzed the impact of Sim2s over-expression in MCF7 cells on the cell cycle and DNA damage response pathways.

CHAPTER II

MATERIALS AND METHODS

Cell Culture

MCF7 cells were maintained in DMEM (Invitrogen, 11965118) supplemented with 10% fetal bovine serum (FBS, Atlanta Biologicals, S11550) and 5% penicillin-streptomycin (Invitrogen 1514-0122). HEK-293 cells were maintained in the same media as described above. Cells were passaged at 70% confluency. All MCF7 cells transduced by viral vectors were maintained in the same media, with an addition of 0.4 $\mu\text{g}/\text{mL}$ puromycin (Amresco J593-25mg).

Lentiviral Transduction

Lentiviral plasmids (pLPCX, Clontech, Sold as part of Catalog # 631511) (Figure 9) were transfected into HEK293 cells, stably expressing Amphotropic envelope proteins, referred to as Ampho 293 cells. Thirty microliters of GeneJuice (Novagen 70967) was added to one milliliter of OptiMEM (Invitrogen, 31985062) and allowed to incubate at room temperature for 5 minutes. Ten micrograms of DNA (a 3:1 ratio of GeneJuice to DNA was used) was added, vortexed, and allowed to incubate at room temperature for 15 minutes. This mixture was added to 10 cm plates of Ampho 293 cells at about 75-80% confluency. Media was changed 24 hours later and the cells were then transferred from 37°C to 32°C. Media was collected at 48 and 72 hours post transfection, filtered through 0.45 μM 50 mL Falcon tubes (Millipore SEIM003M00)

and polybrene was added to a final concentration of 4 $\mu\text{g}/\text{mL}$. Viral media was then added to target cells. The target cells were also incubated at 32°C while undergoing viral infection to promote viral stability. After the infection period was finished, fresh media was added and the cells were returned to 37°C. Selection using puromycin was started 24 hours later. A previous kill curve allowed us to determine the optimal quantity of puromycin to add was 0.4 $\mu\text{g}/\text{mL}$ and selection was continued for seven days.

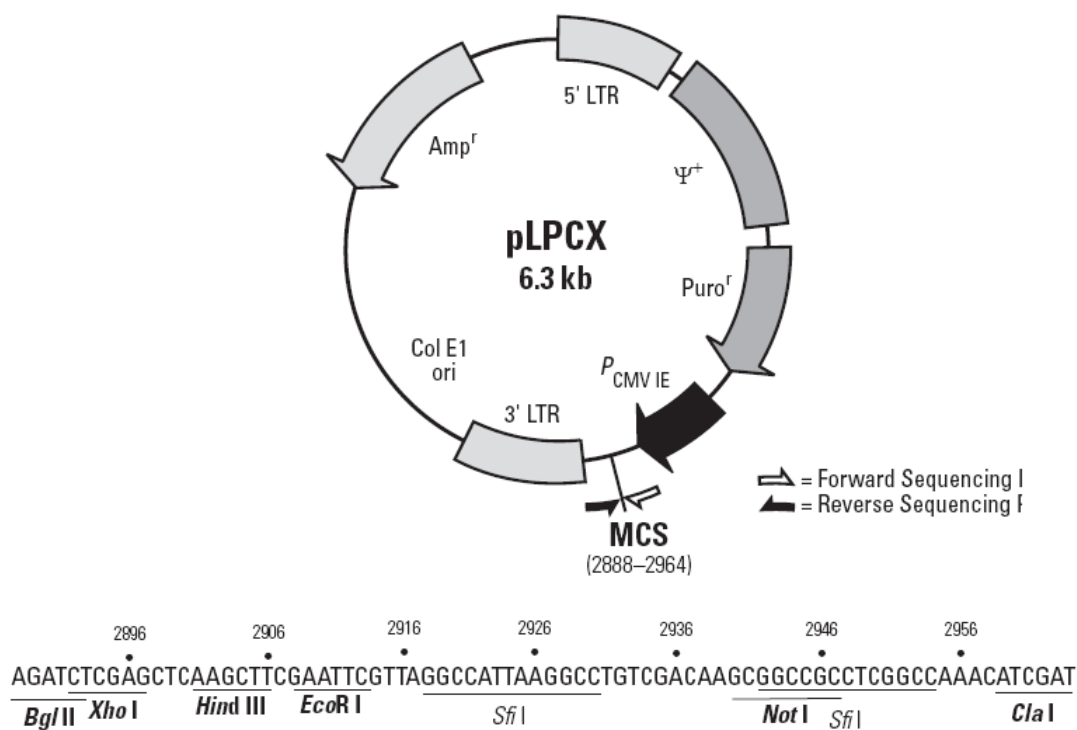


Figure 9. pLPCX vector map. The pLPCX vector was obtained from Clontech. Sim2s was cloned into the MCS between *Bgl* II and *Not* I.

PCR Analysis

RNA Isolation from Cells

Cells were grown to 50-70% confluency, washed with 1xPBS and harvested for RNA using the High Pure RNA Isolation kit (Roche, 11828665001) following the Isolation of Total RNA from Cultured Cells protocol. RNA was eluted in 50 μ L of elution buffer and stored at -80°C .

Reverse Transcription

Depending on the RNA concentration, 0.5-2 μg of RNA was used for reverse transcription reactions. The Transcriptor First Strand cDNA Synthesis kit (Roche, 04379012001) was used. One microliter of Anchored Oligo dT and 2 μL of Random hex primers were added to RNA in H_2O for a total of 13 μL . The sample was incubated at 65°C for 10 minutes, then held at 4°C while 4 μL of TRT 5x Buffer, 0.5 μL RNase inhibitor, 2 μL Deoxy Mix, and 0.5 μL Reverse Transcriptase was added to each sample. Samples went through the following thermocycler program: 25°C for 10 minutes, 50°C for 60 minutes, 85°C for 5 minutes, with a 4°C hold at the end. cDNA was diluted to 20-25 $\text{ng}/\mu\text{L}$ with H_2O and stored at -20°C for long term, and 4°C for immediate use.

Real Time PCR

The following mixture was added to each well of a 96 well plate (Applied Biosystems MicroAmp N801-0560): 20.5 μL of SYBR [FastStart Universal SYBR Green Master (Rox) (Roche, 04913850001)], 2.0 μL cDNA, and 2.5 μL primer mix. Reactions were run according to the following cycle conditions: 95°C for 10 minutes, and 40 cycles of 95°C for 10 seconds followed by 60°C for 1 minute. Analysis was

performed using the $\Delta\Delta\text{CT}$ method. Human TATA-binding protein (TPB) was used to normalize levels of assayed genes. Primer sequences can be found in Table 1.

Table 1. Primer sequences for all Real Time PCR reactions

Gene Name	Sense (5'→3')	Antisense (5'→3')
14-3-3 δ	CAA AGA CAG CAC CCT CAT CAT G	CTC TTC CCC GGC GTT GT
CyclinD1	TGG GTC TGT GCA TTT CTG GTT	GCT GGA AAC ATG CCG GTT AC
E-cadherin	CAC AGA CGC GGA CGA TGA T	GAT CTT GGCTGA GGA TGG TGT AA
FN1	CCA AGA AGG GCT CGT GTG A	GGC TGG AAC GGC ATC AAC
Gadd45	CAA CGA GGA CGC CTG GAA	CGG CTCTCCTCG CAA AAC
GSK-3 β	CTC ATG CTC GGA TTC AAG CA	CAC GGT CTC CAG TAT TAG CAT CTG
MMP1	CCT CGC TGG GAG CAA ACA	TTG GCA AAT CTG GCG TGT ACA
NOXA	CTG CAG GACTGT TCG TGT TCA	GGA ACCTCA GCC TCC AAC TG
p21	CCT AAT CCG CCC ACA GGA A	AAG ATG TAG AGCGGG CCT TTG
p27	GCT AAC TCT GAG GAC ACG CAT TT	CGC ATT GCT CCG CTA ACC
p53	TCT TTG AAC CCT TGCTTG CA	CCG GGA CAA AGC AAA TGG
PUMA	GGG CCC AGA CTG TGA ATC CT	CGT CGCTCT CTC TAA ACC TAT GC
SERBP1	ACG CCT TCA TCT GGG ACA AA	CTA AAA TTC TTT TCT TCG GAG TTT CTT
Sim2s	AAG GTG GGC GGA TCA CCT	CAG CTT CTT GGC AGG CTT G
TBP	TGC ACA GGA GCC AAG AGT GAA	CAC ATC ACA GCT CCC CAC CA

Note: All primers were designed based on mRNA reference from NCBI using Primer Express software (ABI) and purchased from IDT.

Chromatin Immunoprecipitation Assay (ChIP)

Chromatin Harvest

Formaldehyde (Sigma F1635) was added to a final concentration of 1% to fresh culture media. Cells were incubated in this media at room temperature for 10 minutes with gentle rocking. To stop crosslinking, glycine (Sigma G8898) was added to a final concentration of 125 mM and then rocked at room temperature for an additional five minutes. Cells were then washed in ice-cold 1x PBS twice and then scraped in cold PBS containing 25x Complete protease inhibitors (CPI Roche 11-697-498-001) and phosphatase inhibitors [0.05M sodium orthovanadate (Sigma, S6508), 0.25 M sodium molybdate (Aldrich, 243655), 0.5 M sodium fluoride (Sigma, S6776)]. To pellet the cells, they were spun at 805xg for 4 minutes using an Eppendorf 5810R centrifuge chilled to 4°C. To resuspend cells, Nuclear Lysis buffer was added (50 mM Tris pH 8.1, 10 mM EDTA, 1% SDS, 25x Complete protease inhibitors) and then the cells were incubated on ice for 10 minutes. DNA was sheared in 10 second pulses, 10 times, with a one minute pause on wet ice to allow the cells to cool after every 2 pulses. To pellet the cellular debris, the cellular lysate was spun at 16,100 x g in an Eppendorf 5415D centrifuge for 10 minutes at 4°C. Chromatin was stored at -80°C in 60 µL aliquots.

Standard ChIP Assay

ChIP dilution buffer (0.01% SDS, 1.1% Triton X-100, 1.2 mM EDTA, 16.7 mM Tris pH 8.1, 167 mM NaCl, 25x Complete protease inhibitors) was added to one aliquot of chromatin to dilute it 5-fold. To pre-clear the samples 80 µL of salmon sperm DNA/Protein A Agarose (Upstate 16-157) was added and the samples were rocked at

4°C for 30 minutes. Beads were pelleted by spinning at 200 x g for 1 minute in an Eppendorf centrifuge. This step was repeated to complete the pre-clearing. Ten percent of the sample was saved back for input control while the remainder of the sample was split for addition of an antibody and a no antibody control.

The following day, 60 μ L of agarose beads were added for 1 hour at 4°C with rocking. Samples were spun at 2000 x g for 1 minute and supernatant was removed. Beads were washed consecutively for 10 minutes in each solution: Low Salt Wash (0.1% SDS, 1% Triton X-100, 2 mM EDTA, 20 mM Tris pH 8.1, and 150 mM NaCl), High Salt Wash (0.1% SDS, 1% Triton X-100, 2 mM EDTA, 20 mM Tris pH 8.0 and 500 mM NaCl), Lithium Chloride Wash (0.25 M LiCl, 1% NP-40, 1% sodium deoxycholate, 1 mM EDTA, and 10 mM Tris pH 8.0) and twice in TE buffer (10 mM Tris pH 8.0 and 1 mM EDTA). All washes were completed at 4°C except for the TE washes, which were done at room temperature. Immune complexes were eluted from the beads by the addition of 250 μ L Elution buffer (1% SDS and 0.1 M NaHCO₃) vortexing, rocking at room temperature for 15 minutes, then spinning at 14,000 x g for 3 minutes in an Eppendorf centrifuge. Supernatant was removed to a fresh tube, and the process was repeated on the beads for a final volume of elute of 500 μ L. NaCl was then added to a concentration of 0.3 M with 1 μ L of 10 mg/mL RNase-A. Elutes were then incubated at 65°C for 4-5 hours to reverse formaldehyde cross-links. To precipitate the DNA, 2.5 volumes of 100% ethanol was added to each sample and they were placed at -20°C overnight. On the third day, DNA was pelleted by spinning at 14,000 x g in an Eppendorf centrifuge for 10 minutes. Supernatant was removed and the pellet was

resuspended in 100 μ L H₂O. To each sample the following were added: 2 μ L 0.5 M EDTA, 4 μ L Tris, pH 6.5, and 1 μ L 20 mg/mL Proteinase K (Sigma 93161722).

Samples were incubated at 45°C for 1 hour, then purified using a Qiagen PCR purification kit (Qiagen 28106). DNA was eluted in 50 μ L elution buffer (supplied in kit). PCR was performed according to conditions listed in Table 2.

Table 2. Conditions and sequences for ChIP PCR primers

Target	Strand	Sequence	Anneal °C
5' Region of p21	Sense	CCAGGTCTTGGATTGAGGAA	50
	Antisense	TGTTAAGGTGGTGGCATTGA	50
p53 Response Element of p21	Sense	ACATTGTTCCCAGCACTTCC	50
	Antisense	ACACAAGCACACATGCATCA	50
TATA region of p21	Sense	TCTAGGTGCTCCAGGTGCTT	50
	Antisense	ACATTTCCCCACGAAGTGAG	50
Exon 3 Start site of p21	Sense	GTCCGTCAGAACCCATGC	50
	Antisense	CAGGTCCACATGGTCTTCCT	50
Stop region of p21	Sense	CCAAGAGGAAGCCCTAATCC	50
	Antisense	ACAAGTGGGGAGGAGGAAGT	50

Western Blot Assay

Protein Isolation

Cells were washed once with ice-cold 1X PBS and scraped in 2 mL 1X PBS.

Cells were pelleted by spinning at 2000 x g for 4 minutes in an Eppendorf centrifuge.

Supernatant was removed and Lysis buffer [20 mM Tris-Cl pH 8.0, 137 mM NaCl, 10%

glycerol, 1% NP-40, 2 mM EDTA, 25x protease inhibitors, and phosphatase inhibitors was added to resuspend cells. Cells were agitated at 4°C for 30 minutes. Debris was pelleted by spinning in a cooled Eppendorf centrifuge at 14,000 x g for 10 minutes. Aliquots were stored at -20°C, unless they were to be used immediately, in which case they were stored at 4°C. An RC/DC Protein Assay kit (BioRad 500-0120) was used to ascertain protein concentration.

Standard Analysis

After determining the amount of protein to add for a certain concentration, samples were QS'd to 30 μ L with H₂O and 6 μ L of 6x SDS loading buffer (60% glycerol, 0.3 M Tris pH 6.8, 12 mM EDTA, 12% SDS, 6% β -mercaptoethanol, 0.5% bromophenol blue) was added and samples were boiled for 5 minutes, followed by 5-10 minute incubation on wet ice. Acrylamide gels ranging from 8-12% were cast for analysis. Gels were run at 110 mV (constant V) for 1-2 hours and transferred to PVDF membranes for 2 hours at 110 mA (constant mA). Depending on antibody conditions membranes were blocked in either PBS-T + 5% milk (BioRad 170-6404) or TBS-T + 5% milk. All primary antibodies were incubated at 4°C over night, while gently rocking. See Table 3 for antibody sources and incubation conditions. Proteins were visualized with the Amersham ECL Plus western blotting detection reagent (GE Healthcare RPN 2132) on film (HyBlot CL Autoradiography film, Denville Scientific, L3018). Films were developed on a Kodak M35a X-omat film processor. All films were scanned using a Dell All-in-One scanner.

β -Galactosidase Staining

Cells were plated in six-well plates two to three days prior to use. Cells to be treated with UV or sham were treated, and then six hours later stained for β -galactosidase [Senescence beta-Galactosidase Staining kit (Cell Signaling, 9860)]. The cells were washed with 1X PBS twice; then treated with the 1X Fixative solution for 15 minutes at room temperature. After incubation, cells were washed with 1X PBS twice, and then treated with the 1X Staining solution as described in the kit protocol. The Staining solution was equilibrated to pH 6.0 and the cells were incubated at 37°C overnight in a ProBlot 6 Hyb oven. Cells were imaged on SteREO Discovery.V12 microscope at various magnifications.

Clonogenic Survival Assay

Plating Cells

To plate equal numbers of cells, cellular media was removed, cells were rinsed with 5 mL 1X PBS, and 2 mL 0.5% trypsin-EDTA was added. Cells were re-suspended in 8 mL media to neutralize trypsin. Cells were vigorously pipetted to break up clumps, then 100 μ L of this solution was added to 20 mL isotonic solution to be counted on a Beckman Coulter Z1 Coulter Particle Counter. Cells were plated at 5000 cells/well in a 6-well plate. Cells were allowed to settle and adhere to the plate for 2 hours, at which point they were treated with 2000 μ J/m² UV. Cells were incubated at 37°C for 6 hours, then fixed and stained.

Table 3. Conditions for antibodies used

Antibody	Company/Cat. #	Dilution	Amt. protein	Washes/Milk	Secondary	Company/Cat. #	Dilution
Rb α ACH3	Millipore/06-599	(1:2000)	10	0.1% TBS-T/TBS-T 5% milk	Dk α Rb	Santa Cruz/sc-2313	(1:5000)
Ms α B-Actin	Sigma/A5441	(1:7000)	10	0.05% PBS-T/PBS-T 5% milk	IgG α Ms	Upstate/12-349	(1:4000)
Rb α cdc2	Millipore/15-120	(1:1000)	50	See product information	Dk α Rb	Santa Cruz/sc-2313	(1:5000)
Rb P-cdc2	Santa Cruz/12340-R	(1:500)	50	0.1% TBS-T/TBS-T 5% milk	Dk α Rb	Santa Cruz/sc-2313	(1:4000)
Rb α cdc25A	Santa Cruz	(1:500)	150	0.1% TBS-T/TBS-T 5% milk	Dk α Rb	Santa Cruz/sc-2313	(1:5000)
Rb α Cyclin A	Santa Cruz/sc-596	(1:800)	50	0.1% TBS-T/TBS-T 5% milk	Dk α Rb	Santa Cruz/sc-2313	(1:5000)
Ms α Cyclin B1	Millipore/15-120	(1:1000)	50	See product information	IgG α Ms	Upstate/12-349	(1:4000)
Rb α Cyclin E	Neomarkers/RB-012-PO	(1:1000)	50	0.1% TBS-T/TBS-T 5% milk	Dk α Rb	Santa Cruz/sc-2313	(1:5000)
Rb α cleaved caspase 9	Cell Signaling/9501	(1:500)	75	0.1% TBS-T/TBS-T 5% milk	Dk α Rb	Santa Cruz/sc-2313	(1:5000)
Rb α Gadd45 α	Santa Cruz/SC-797	(1:500)	10	0.05% PBS-T/PBS-T 5% milk	Dk α Rb	Santa Cruz/sc-2313	(1:5000)
Rb α GSK3B	Cell Signaling/9323	(1:1000)	150	0.05% PBS-T/PBS-T 5% milk	Dk α Rb	Santa Cruz/sc-2313	(1:5000)
Ms α H3K9Me2	AbCam/ab1220	(1:500)	75	0.05% PBS-T/PBS-T 5% milk	IgG α Ms	Upstate/12-349	(1:4000)
Ms α Hsp90	Stressgen/SPA-830	(1:500)	50	0.1% TBS-T/TBS-T 5% milk	IgG α Ms	Upstate/12-349	(1:5000)
Rb α Ki67	Neomarkers/RM-9106	(1:500)	50	0.05% PBS-T/PBS-T 5% milk	Dk α Rb	Santa Cruz/sc-2313	(1:5000)
Ms α p21	Dako Cytomation/9286	(1:700)	150	0.05% PBS-T/PBS-T 5% milk	IgG α Ms	Upstate/12-349	(1:4000)
Gt α p53	R&D/1355	(1:1000)	10	0.1% TBS-T/TBS-T 5% milk	Dk α Gt	Santa Cruz/sc-2033	(1:4000)
Rb α P-p53	Cell Signaling/9286	(1:1000)	100	0.05% PBS-T/PBS-T 5% milk	Dk α Rb	Santa Cruz/sc-2313	(1:5000)
Rb α PARP	Cell Signaling/9541	(1:1000)	50	0.1% TBS-T/TBS-T 5% milk	supplied in kit		
Rb α Retinoblastoma	Santa Cruz/sc-50	(1:500)	150	0.1% TBS-T/TBS-T 5% milk	Dk α Rb	Santa Cruz/sc-2313	(1:5000)
Rb α Sim2s	Millipore/AB4145	(1:700)	150	0.05% PBS-T/PBS-T 5% milk	Dk α Rb	Santa Cruz/sc-2313	(1:5000)

Fixing and Staining Cells

The cell media was removed and cells were rinsed with 1 X PBS. Two millileters of 3.0% gluteraldehyde and 0.5% crystal violet was added to each well of the six-well plates and plates were incubated for 60 minutes at room temperature. The gluteraldehyde/crystal violet mixture was removed from each well and plates were carefully rinsed by immersing in a sink filled with room temperature tap water. Plates were turned upside down and allowed to dry at room temperature over-night.

Analysis

ImageJ 1.42q was used to analyze stained cells. After taking pictures of the cells on a SteREO Discovery.V12 microscope, images were opened in Image J.

Process→Binary→Make Binary edited the pictures to black and white.

Analyze→Analyze particles allowed the program to count individual cells. Pixel size had to be adjusted to the smallest size allowable for the program to count, this number was maintained for all images counted at the same magnification.

Proliferation Assay

Cells were counted as mentioned above and then plated 5000/well into the wells of 6-well plates. Cells were counted from one well each day for 7 days. The count was done in triplicate each day.

Flow Cytometry

Preserving Cells

Falcon tubes (15 mL) were filled with 4.5 mL of ice-cold 70% EtOH and kept on ice. Cells were harvested at 75-80% confluency using 0.5% Trypsin-EDTA. Cells were centrifuged at 250xg for 3 minutes, the supernatant was removed, and the cells were resuspended in 500 μ L 1X PBS. The resuspended cells were vortexed vigorously to break up any cell clumps, and transferred to the chilled tubes of 70% EtOH and vortexed vigorously again. Cells were stored at -20°C until use.

Staining Cells

Because MCF7 cells break down and clump so easily, a propidium iodide (PI) solution containing no detergent was optimized. A hypotonic solution containing sodium citrate allowed the propidium iodide to incorporate into the nucleus without over-damaging cells. The stock solutions used to create the PI solution are as follows: Sodium citrate (11.76 mg/mL), Propidium iodide (1.0 mg/mL), RNaseA (2.0 mg/mL). The final concentrations required in the PI solution are as follows: Sodium Citrate (4 mM), PI (50 μ g/mL), RNaseA (200 μ g/mL).

Preserved cells in 70% EtOH were spun down at 500xg for five minutes, and the supernatant was removed. Cells were rinsed in 1X PBS, allowed to rest for 60 seconds, then spun at 500xg for five minutes. The supernatant was removed again and the cells were resuspended in one millileter of the PI solution. Cells were vortexed vigorously to prevent clumping, and incubated at RT for 20 minutes. Cells were then placed on ice and transported to the Flow Cytometer.

Analysis

Cells were run on a FACSCalibur (Becton Dickinson Immunocytometry Systems) and then analyzed using ModFit LT, version 3.2 for Macintosh (Verity Software House, Topsham, MA).

DIC Imaging

Differential interference contrast images of MCF7 pLPCX-Sim2s and -Empty cells were captured with a Zeiss Stallion Dual Detector Imaging System with Intelligent Imaging Innovations Software (Carl Zeiss Inc., Thornwood, NY).

Statistical Analysis

Results referred to in the remaining text are expressed as mean \pm SEM. Data were analyzed by Student's *t* test. *P* values of <0.05 were considered significant.

CHAPTER III

THE ROLE OF SIM2S IN CELL CYCLE REGULATION

Our laboratory has previously shown that over-expression of Sim2s in MDA-MB-435 cells results in decreased proliferative and invasive potential of this normally highly invasive breast cancer cell line. Additionally, when Sim2s is knocked down in the less invasive MCF7 breast cancer cell line it increases their invasive and proliferative potential and creates an EMT-like phenotype (18).

To further investigate the role of Sim2s as a tumor suppressor, we over-expressed Sim2s in MCF7 cells using a lentiviral system. Similar to the MB-MDA-435 cells, we found that Sim2s decreased cell proliferation (Figure 10).

Because of this decreased proliferation we investigated the possibility that these cells were arresting at a particular stage of the cell cycle by performing propidium iodide flow cytometry. The results show that there is significant accumulation of cells in G2/M and S phases of the cell cycle in MCF7-Sim2s cells compared to Empty controls (Figure 11). Western blot analysis of the cyclins and CDKs involved at these cycle checkpoints found no differences in expression levels (Figure 12).

Because we observed no differences at this level, we looked at RNA expression levels of regulatory factors involved in monitoring cell cycle regulation. We surveyed several regulatory proteins involved in arrest at G2/M including 14-3-3 δ , GSK3- β , and GADD45. While there was no change in 14-3-3 σ or GSK3- β , GADD45 mRNA was up-regulated. However, Western blot analysis showed no up-regulation at the protein level for GADD45 (Figure 13). As a control we measured p27 mRNA levels (a protein

involved in regulating cell cycle arrest at the G1 stage) and found no change in expression of this gene.

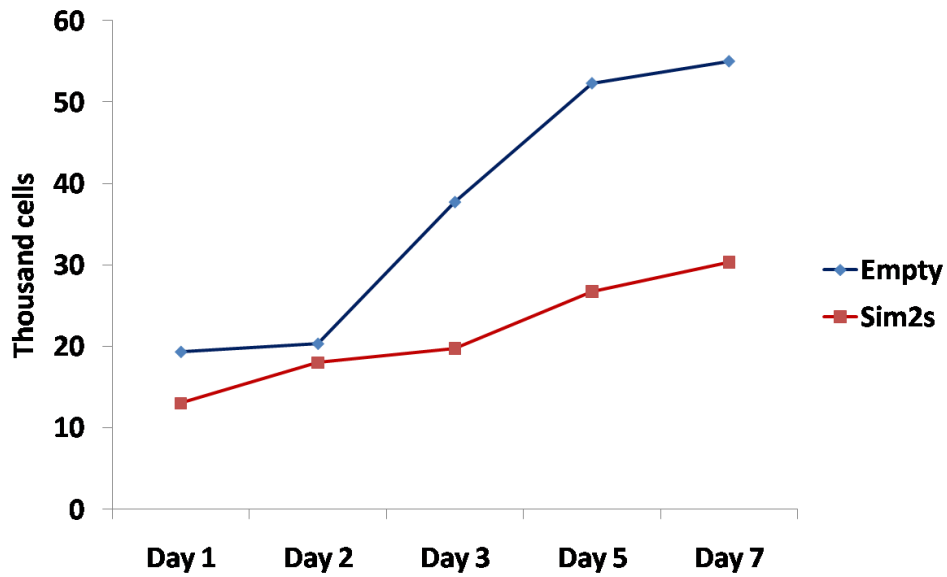


Figure 10. Proliferation assay on MCF7 pLPCX-Empty and Sim2s cells. Sim2s cells are less proliferative than their control counterparts.

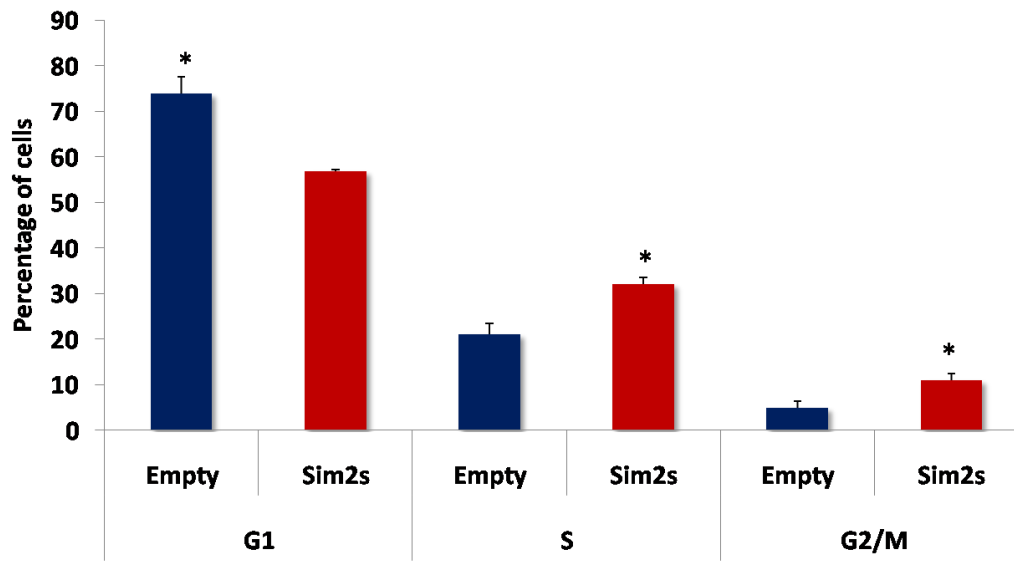


Figure 11. Propidium iodide flow cytometry of MCF7 pLPCX Empty and Sim2s cells. Significantly more Sim2s over-expressing MCF7 cells are found in the G2/M and S phases of the cell cycle. Columns represent mean recorded cells, (n=18); bars, SEM, *, P<0.003.

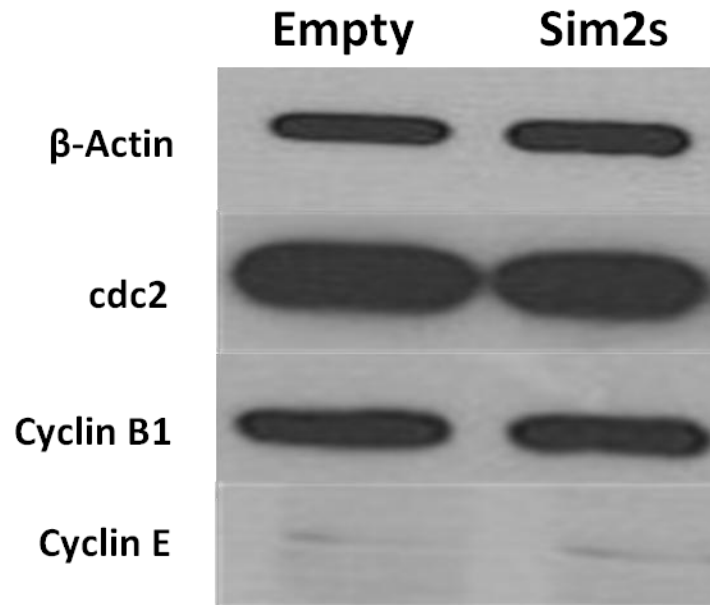


Figure 12. Western blot analysis of major cyclins and CDKs involved in cell cycle. Because MCF7 cells over-expressing Sim2s arrest in G2/M and S phase, cyclins and CDKs involved in these phases of the cell cycle were surveyed. Equal amounts of protein were loaded and subjected to immunoblotting. There was no discernable change in expression levels of any of these cell cycle proteins between Empty and Sim2s cells. Figure is representative of three separate trials.

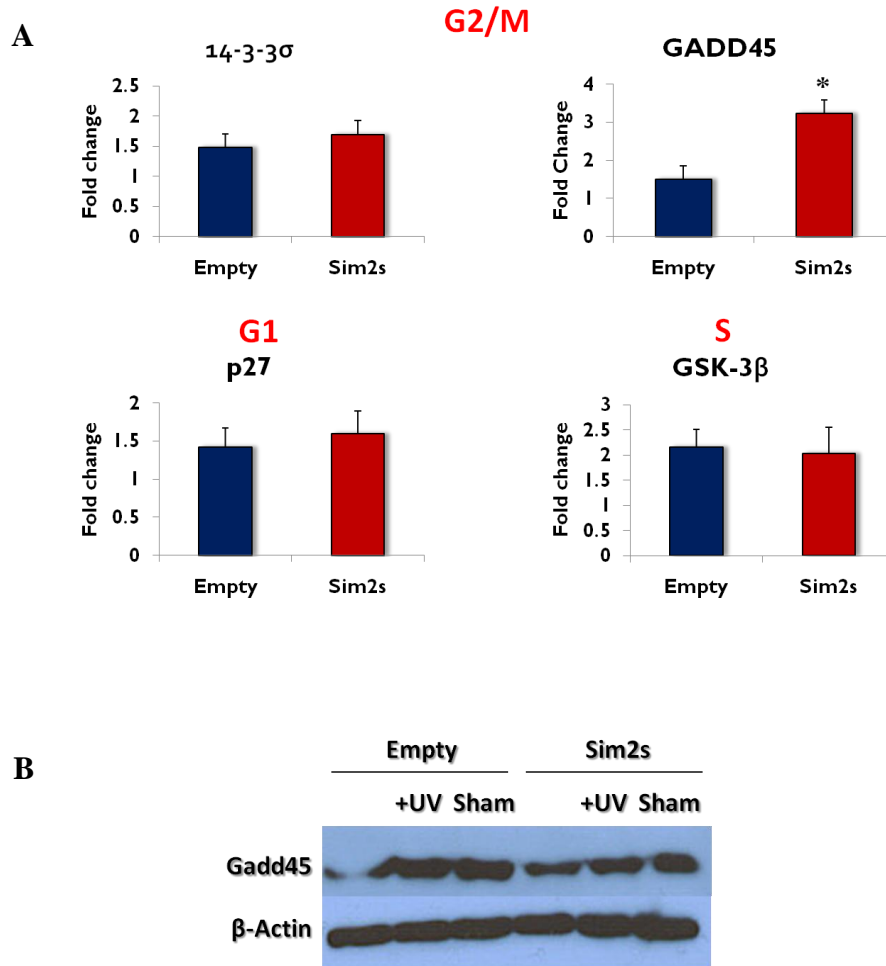


Figure 13. Real Time PCR assay of expression levels of regulatory protein RNA levels and Western blot analysis of GADD45. **A.** Cell cycle regulatory proteins from the G2/M phase of the cell cycle were surveyed to investigate if up-regulation of Sim2s resulted in concomitant up-regulation of these proteins. Only GADD45 showed significant up-regulation with over-expression of Sim2s, but was not up-regulated at the protein level. As a control, p27, a regulatory protein involved in G1 arrest was surveyed. No change was noted between Sim2s and Empty controls. **B.** Western blot analysis of Gadd45 showed no change between Empty and Sim2s. For all Real Time PCR analyses, expression levels are relative to TBP expression, (n=3); bars, SEM; *, P<0.05. For Western blot analysis, equal amounts of protein were loaded and subjected to immunoblotting. Figure is representative of three separate trials.

CHAPTER IV

THE ROLE OF SIM2S IN DNA DAMAGE RESPONSE AND CELLULAR SENESCENCE

In addition to being closely linked with the G1 checkpoint, p21 is also involved in regulating several other checkpoints in the cell cycle, including the G2/M and S phases. To determine if the G2/M arrest observed in MCF7 cells over-expressing Sim2s is associated with changes in p21, we analyzed p21 expression levels. The results show that over-expression of Sim2s significantly increased p21 basal levels at both the RNA and protein levels, suggesting that the G2/M arrest may be p21 dependent (Figure 14).

Previous studies have shown that down-regulation of Sim2s in MCF7 cells by shRNA (Sim2si) induces an EMT characterized by increased proliferation and invasion both *in vitro* and *in vivo* (18). Analysis of p21 expression in control and Sim2si MCF7 cells showed that loss of Sim2s corresponds to a decrease in basal p21 expression at the RNA and protein levels (Figure 15). This trend is also observed in response to DNA damage in the form of doxorubicin exposure: Scr cells show a significant increase in p21, while Sim2si show little response. In contrast, exposing Empty and Sim2s cells to UV radiation dramatically increases p21 expression.

In addition to p21, changes in p53 levels were investigated to ascertain whether the differences in p21 expression required activation of p53. When Sim2s is knocked-down in MCF7 cells, p53 protein (but not RNA) levels increase dramatically, regardless of exposure to DNA damage. However, in MCF7-Sim2s cells, while active p53 levels

increase upon exposure to DNA damage, the change is no different from that of Empty control cells. There is no dramatic difference in phospho-p53 levels with Sim2s over-expression, suggesting that the up-regulation of p21 by Sim2s is p53-independent (Figure 15).

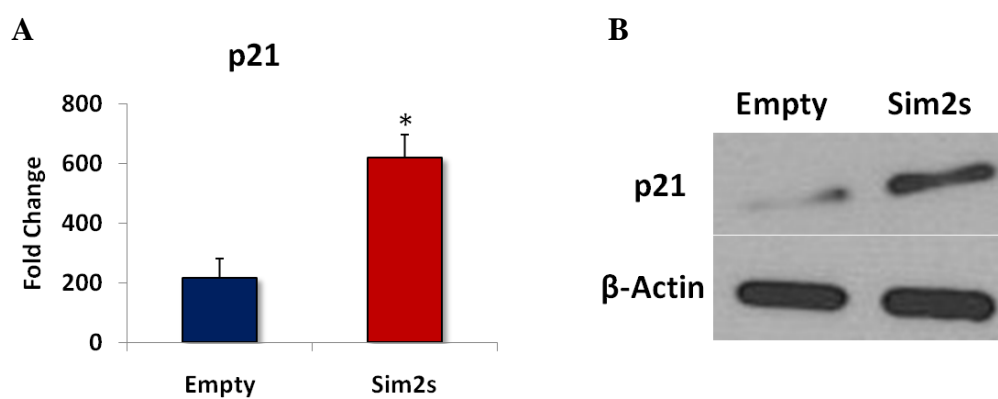


Figure 14. Real Time PCR assay and Western blot analysis of p21. **A.** Expression levels of p21 were also analyzed and found to be significantly up-regulated in Sim2s cells at both the RNA and protein levels. **B.** Real Time PCR analysis, expression levels are relative to TBP expression, (n=3); bars, SEM; *, P<0.05. Western blot representative of three separate trials.

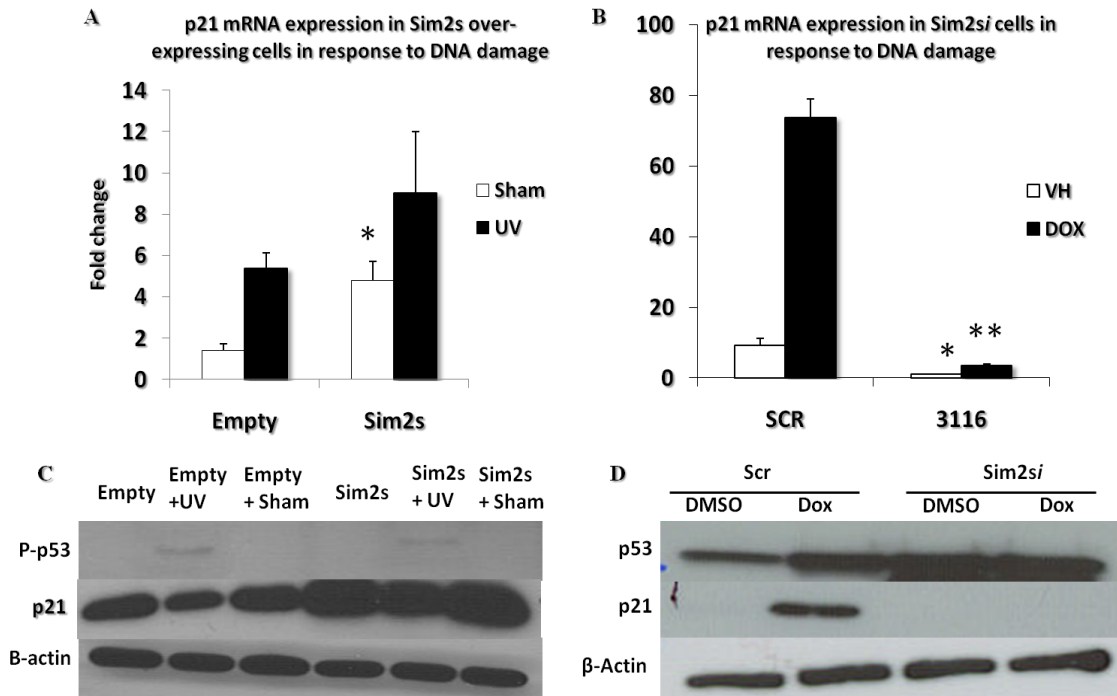


Figure 15. Over-expression of Sim2s regulates p21 expression in response to DNA damage. **A**. MCF7 cells over-expressing Sim2s have significantly higher p21 RNA levels than Empty control cells. This trend continues with exposure to 5000 $\mu\text{J}/\text{m}^2$ UV. **B**. Previous work in our laboratory has shown that knock-down of Sim2s results in almost complete ablation of p21 RNA expression. **C**. In MCF7 cells that have had Sim2s over-expressed, protein expression of p21 is greater, regardless of both exposure to DNA damage, and phospho-p53 levels as compared to Empty control cells. **D**. Western blot confirms that p21 expression is not seen in Sim2si cells, even though there is increased p53 expression. UV=5000 $\mu\text{J}/\text{m}^2$, Sham=sham irradiation, VH=DMSO, DOX=treatment with 1 μM doxorubicin for 12 hours. For all Real Time PCR analyses, expression levels are relative to TBP expression, (n=3); bars, SEM; *, P<0.05. For Western blot analysis, equal amounts of protein were loaded and subjected to immunoblotting.

Our lab previously demonstrated that basal and DNA damage induced p21 expression is Sim2s dependent (Figure 15). Because p21 plays such a major role in response to genotoxic stress, we exposed MCF7 Empty control and Sim2s cells to 1000 μ J UV and measured changes in proliferation using a clonogenicity assay. As expected, MCF7-Sim2s cells grew at a slower rate compared to controls and this response was further exacerbated in response to UV irradiation (Figure 16).

This loss of clonogenicity has been shown previously with up-regulation of p21. Chang et al. showed that over-expression of p21 from an inducible promoter resulted in a senescent-like growth arrest in a human fibrosarcoma cell line. After release from this growth-arrest, cells re-entered the cell cycle but showed growth retardation, cell death, and decreased clonogenicity (37).

Because Sim2s is a transcription factor we performed a Chromatin Immunoprecipitation (ChIP) assay to determine if Sim2s binds the p21 gene. Chromatin was harvested from WT MCF7 cells treated with either 5000 μ J UV or sham and pulled down using a Sim2s antibody. Using primers located across the p21 gene we looked to see if Sim2s was bound at any of the locations (5' region of the gene, p53 Response element, TATA region, ATG start of exon 3, or the Stop region) surveyed. In response to UV radiation, Sim2s binds to p21 at the 5' region of p21, the p53 Response element, and the ATG start site of exon 3 (Figure 17).

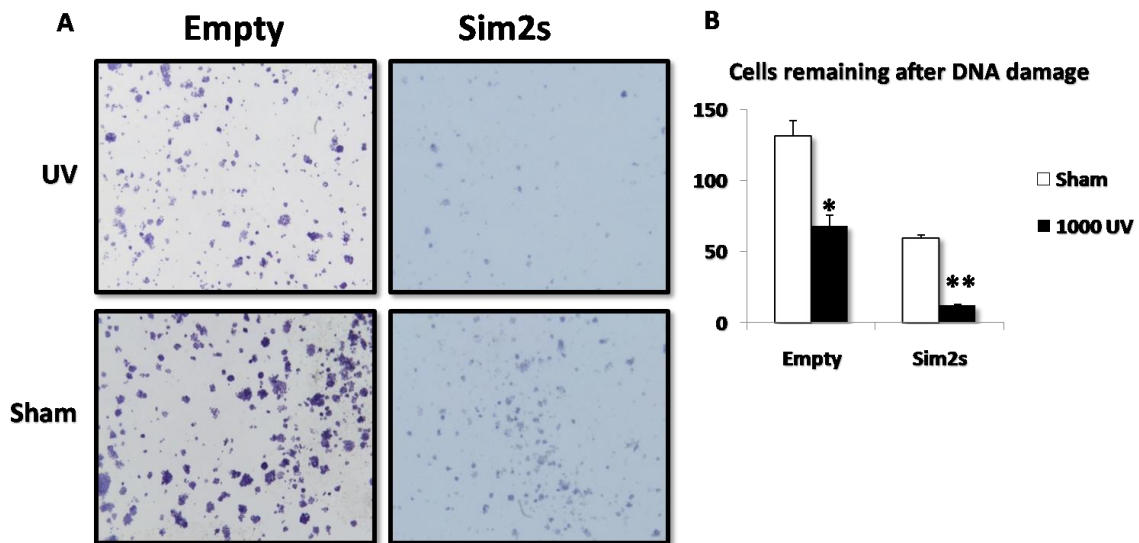


Figure 16. Clonogenic survival assay of MCF7 pLPCX-Empty and Sim2s cells to ascertain survival upon exposure to genotoxic stress. **A**. Crystal violet staining. The same number of cells was plated for both Sim2s and Empty controls and then treated with 1000 μ J UV. After seven days, cells were fixed, and stained with crystal violet. **B**. Cells were analyzed using ImageJ to determine how many cells had survived the initial genotoxic stress. Sim2s cells are less proliferative overall, but appear to be more sensitive to UV treatment. Cell count analysis ($n=3$); bars, SEM; *, $P<0.005$, **, $P<0.0009$.

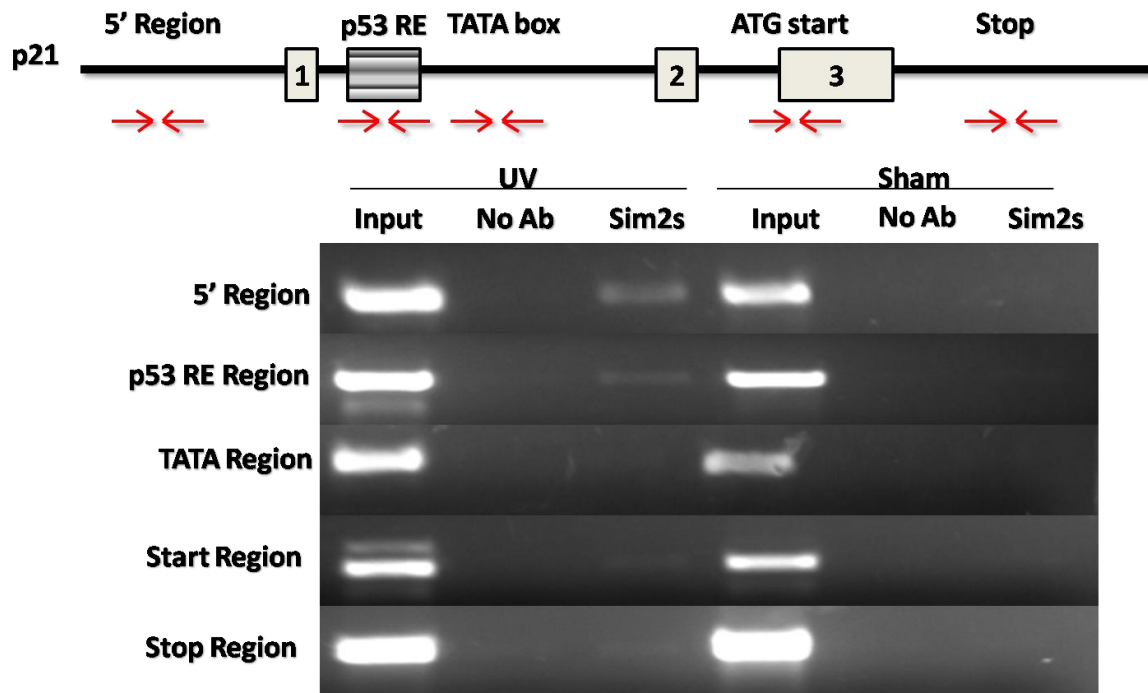


Figure 17. ChIP analysis of MCF7 pLPCX-Empty and Sim2s cells upon exposure to UV radiation. Because p21 is often up-regulated in response to DNA damage, MCF7 cells were treated with $5000\mu\text{J}/\text{m}^2$ UV. ChIP assay shows that Sim2s binds to the p21 gene at the 5' region, p53 Response Element, and to a small extent at the ATG start site of Exon 3. This binding is only seen with UV treatment.

In addition to arresting cells at various stages of the cell cycle, p21 also plays an important role in promoting cellular senescence. Because of the significant inhibition of proliferation observed in Sim2s over-expressing cells, we needed to determine if the cells were not only arresting, but actually undergoing cellular senescence. Our initial observations of morphological differences showed that Sim2s over-expressing cells had the characteristic “fried-egg” appearance of senescent cells (Figure 18).

Additionally, we performed a β -galactosidase stain to confirm senescence and the increased β -galactosidase activity observed in the Sim2s cells is a positive indication of senescence (Figure 19). To further confirm the senescence phenotype, we analyzed changes in Ki67, a nuclear marker highly expressed in actively proliferating cells, but in lower levels in cells undergoing senescence; and H3K9Me2, a histone marker often found in higher quantities in senescent cells, but not in cells actively proliferating. Western blot analysis shows that Sim2s cells had decreased levels of Ki67 and an increase in H3K9Me2 levels—further confirming that these cells are undergoing senescence (Figure 20). Additionally, we found that Sim2s cells increased levels of cleaved Poly (ADP-Ribose) polymerase (PARP) a protein associated with apoptosis.

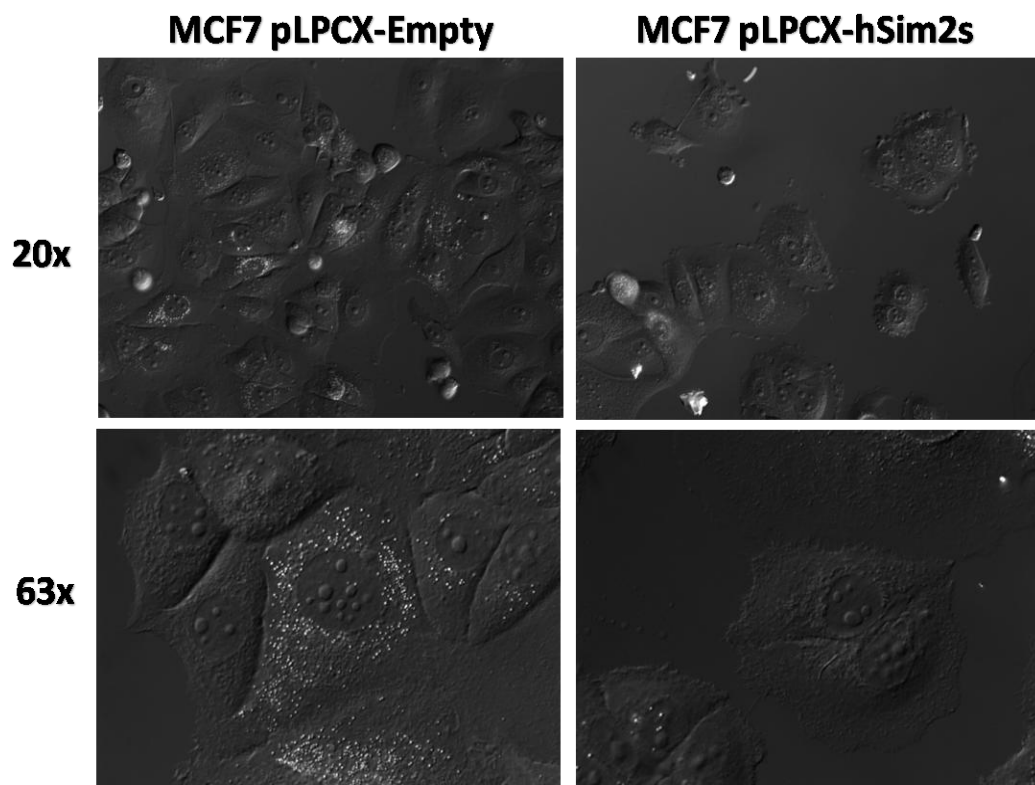


Figure 18. DIC images of Sim2s over-expressing MCF7 cells and Empty controls. Sim2s cells (on the right) show classic “fried-egg” appearance characteristic of senescence.

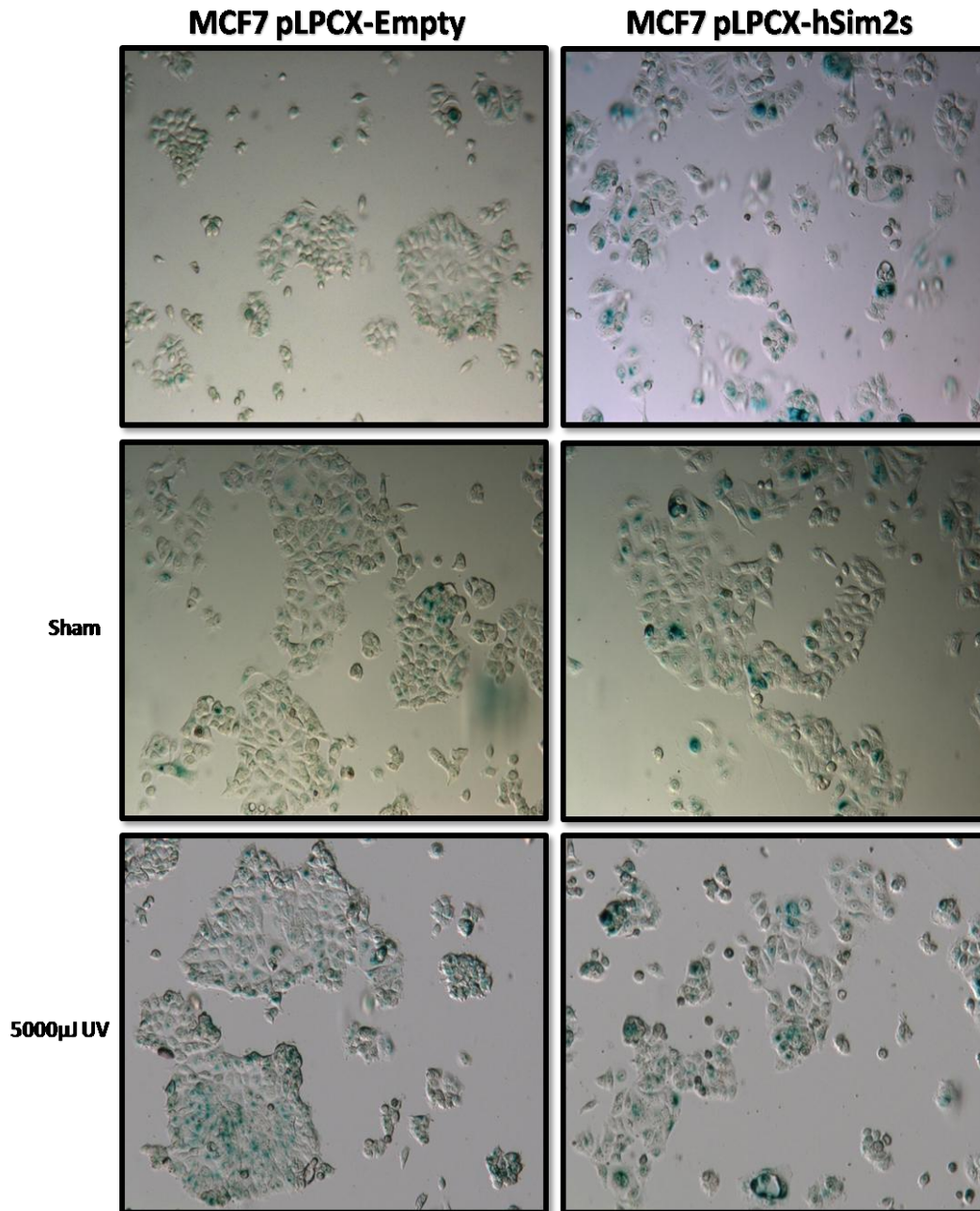


Figure 19. MCF7 pLPCX-Sim2s cells have increased β -galactosidase staining as compared to Empty controls. This is seen with no treatment (top two panels), sham treatment (middle two panels), and 5000 μ J UV treatment (bottom two panels). This increased staining is seen by the dramatic, deep blue color seen in the Sim2s cells.

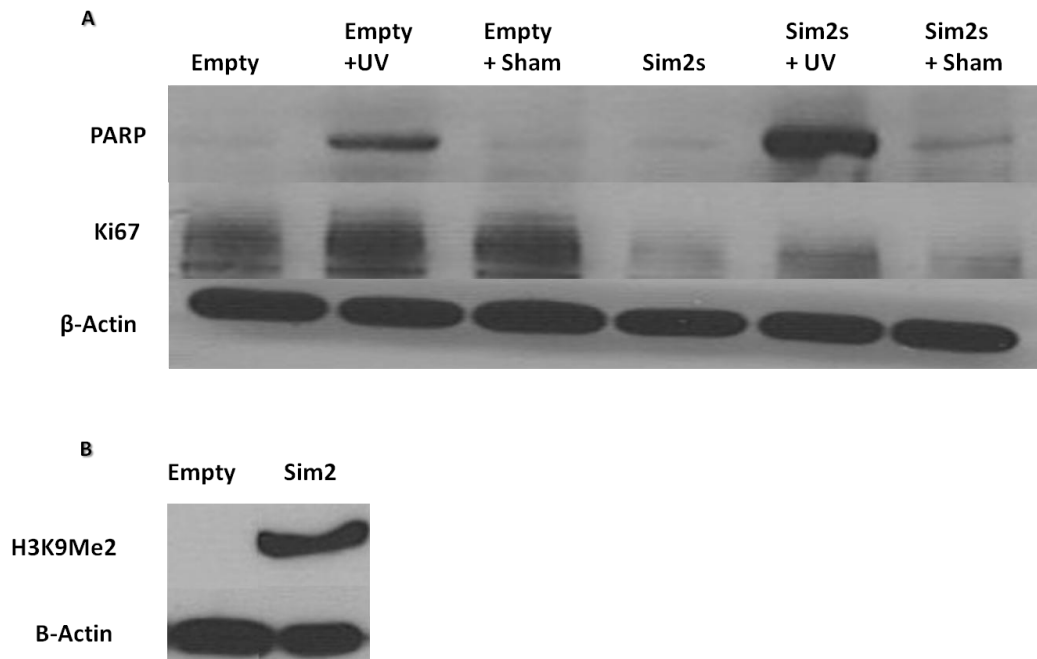


Figure 20. Western blot analysis of cell proliferation marker Ki67 and apoptotic marker PARP. **A.** Empty cells have higher levels of the nuclear marker Ki67 indicating a higher level of proliferative activity as compared to Sim2s cells. PARP levels are higher in Sim2s cells however, indicating that these cells are also undergoing increased apoptosis—in addition to their increased cellular senescence. **B.** A different Western blot shows the histone marker H3K9Me2, generally associated with decreased activity (decreased proliferation) is seen to be up-regulated in MCF7 cells over-expressing Sim2s. Equal amounts of protein were loaded and subjected to immunoblotting. Results shown are representative from two trials in A, but only one trial in B.

CHAPTER V

CONCLUSIONS

In *Drosophila*, the *Singleminded* gene is responsible for cell fate determination in central nervous development and during embryogenesis (3, 38). Because of its location in the Down Syndrome Critical Region of Chromosome 21 and the decreased incidence of breast cancer seen in these individuals, our laboratory was interested in determining the role Sim2 plays in breast cancer. We were the first to determine the role of the short isoform of Sim2, Sim2s, in normal development of the mammary gland and the requirement of Sim2s in maintaining epithelial cell fate in breast cancer cells (18). Additionally, we have shown that precocious expression of *Sim2s in vivo* promotes an alveolar epithelial cell phenotype with an increase in a subset of milk protein genes (9). Based on these studies, we hypothesized that Sim2s has tumor suppressive activity and that over-expression of Sim2s in MCF7 cells will result in cell cycle arrest and sensitization to DNA damaging reagents.

To test this hypothesis, we used a lentiviral vector to over-express Sim2s in MCF7 cells. We have previously reported that over-expression of Sim2s in MDA-MB-435 cells resulted in decreased proliferation. This was also observed with over-expression of Sim2s in MCF7 cells (Figure 9). To determine if this decreased proliferation is the result of a cell cycle arrest, propidium iodide flow cytometry was performed and significantly more Sim2s over-expressing cells were found in G2/M and S phase of the cell cycle (Figure 10). After characterizing the cyclin and CDK activity

for Sim2s over-expressing cells and Empty controls we found that there were no changes in expression of critical cell cycle regulations (Figure 11) which led us to conclude that Sim2s is not causing cell cycle arrest by directly influencing expression levels of the cyclins and CDKs involved in S and G2/M phase (cyclin A, E and B1 and CDK1). However, to fully determine if this is the case, a survey of phosphorylated cyclins and CDK or a kinase activity assay should be done.

Before examining this further, we investigated whether Sim2s over-expression influenced expression of regulatory proteins. The key regulatory G2/M proteins 14-3-3 σ and GADD45 α play roles in influencing a G2/M arrest (39). Upon activation, 14-3-3 σ binds to Cdc25c, sequestering it in the cytoplasm, thus inhibiting subsequent binding to Cdc2, ultimately preventing the cell from moving through G2 into M phase. Activation of GADD45 α causes cell cycle arrest at the G2/M phase by directly interacting with Cdc2 and causing it to dissociate from Cyclin B. Additionally, GADD45 α can directly interact with p21, inducing cell cycle arrest via p21 interaction with cell cycle proteins. Because all of these regulatory proteins work by merely causing dissociation, but not down-regulation of the cell cycle proteins, we hypothesized that the effects of Sim2s on cell cycle arrest was due to interaction with one or more of these regulatory proteins. We surveyed mRNA levels of these three major regulatory proteins and found no difference in expression between MCF7 Empty control and Sim2s cells, suggesting that other pathways are required to mediate Sim2s-dependent cell cycle arrest. However, to truly ascertain differences in expression, since G2 arrest is caused by protein activation, not necessarily up-regulation of gene expression, Western blot analysis of all three

regulatory proteins will need to be done. GADD45 α was analyzed via Western blot, and no significant difference in protein levels between Sim2s and control cells was observed.

The cyclin-dependent kinase inhibitor p21 plays an essential role in DNA damage response, by inducing cell cycle arrest, inhibiting DNA replication and by regulating key apoptotic processes. The ability of p21 to interact with a number of proteins involved in these processes is extremely important. We found that over-expression of Sim2s results in up-regulation of p21 and we hypothesize that either individually, or in direct interaction with p21 results in the observed G2/M cell cycle arrest. However, to investigate this hypothesis we will need to perform a CoIP and/or ChIP to show interaction between p21 and Sim2s.

In contrast to the up-regulation of p21 observed with over-expression of Sim2s in MCF7 cells, previous work in our lab has shown that in cells that have had Sim2s knocked down (Sim2si cells), p21 expression is ablated—even in response to DNA damage, which is usually a strong stimulus for p21 activation (40) (Figure 13). Because DNA damage usually results in p53 activation, we were interested in determining p53 expression in the case of Sim2s knock-down and over-expression.

In Sim2si cells levels of p53 increased regardless of DNA damage (UV radiation). However, this was not accompanied with increased p21 expression. In contrast, in the Sim2s over-expressing cells, p53 levels only increased in response to DNA damage, whereas p21 levels were significantly higher in all cells over-expressing Sim2s (Figure 15). In both cases, the p21 response appears to be p53-independent. The p53 response observed in the Sim2si cells is extremely interesting and we hypothesize

that Sim2s could play a role in activating or interacting with p53 in addition to p21. Because of the role p53 and p21 both play in cellular response to DNA damage through arrest or apoptosis, it is important to further delineate the mechanism through which Sim2s affects the observed cellular senescence.

To investigate if over-expression of Sim2s and the resulting up-regulation of p21 affected cells viability, we exposed MCF7 cells to UV radiation. We hypothesized that Sim2s-mediated up-regulation of p21 would result in sensitization to genotoxic reagents and thus a decrease in cell proliferation/survivability. After exposure to 1000 μ J of radiation, cells were grown for one week and stained to assay clonogenicity. In support of our hypothesis, Sim2s over-expressing cells were indeed sensitized to DNA damage (Figure 14). This result was interesting because of the role p21 plays in cell cycle arrest. To investigate this process further we wanted to determine if p21 was playing a role in inducing cellular senescence and causing the observed cell cycle arrest. First, however, we performed a ChIP analysis to determine if Sim2s can interact with p21. Using five sets of primers spread across the p21 gene, we assayed for Sim2s binding in normal MCF7 cells. We found that Sim2s does bind to p21 at the 5' region of the gene, TATA box region, and at the ATG start of Exon 3 (Figure 15). This observation was only detected when cells had been exposed to DNA damage (UV radiation). This suggests that Sim2s can bind the p21 promoter and potentially induce activation of this gene in response to DNA damage resulting in the observed cell cycle arrest.

The observed cell cycle arrest was further investigated to determine if the cells were undergoing senescence. DIC imaging was used to compare gross morphology.

This confirmed what was observed under less magnification: cells over-expressing Sim2s are larger with frilled edges—resembling the “fried-egg” appearance characteristic of senescent cells (Figure 16). To confirm senescence we performed several different assays. Sim2s over-expressing cells and Empty controls were stained for β -galactosidase activity and a significant increase in this activity (indicative of cellular senescence) was noted in Sim2s over-expressing cells (Figure 17). Other markers that are indicative of a senescence status were also evaluated. Ki67 (a nuclear antigen found in actively proliferating cells) expression is found in higher levels in Empty controls as compared to Sim2s over-expressing cells. Additionally, we looked at the histone marker H3K9Me2 which is generally associated with a closed conformation, indicative of decreased transcriptional activity and cell proliferation. Western blot analysis shows that Sim2s over-expressing cells have increased levels of this repressive histone marker, compared to Empty controls (Figure 18). Based on these assays, we concluded that Sim2s cells are indeed undergoing senescence; most likely due to the up-regulation of p21 as a result of over-expression of Sim2s. In addition to induction of cellular senescence, we observed an increase in cleaved PARP expression in Sim2s over-expressing cells. Due to this up-regulation, we conclude that not only are these cells undergoing senescence, but are also undergoing increased apoptosis—which is perhaps indicative of their increased sensitivity to DNA damaging reagents. The increased observed cellular senescence is interesting when tied back to DS, as this genetic disorder is associated with many signs of premature tissue aging including T-cell deficiency, and increased incidence of early Alzheimer type (41). Increased cellular senescence has

been tied to aging, including disorders such as Alzheimer's and Parkinson's disease (42) and cancer (43).

These results suggest a model in which over-expression of Sim2s regulates the cell cycle regulatory protein, p21, causing an arrest in the G2/M phase of the cell cycle. Additionally, up-regulation of p21 results in increased cellular senescence as shown by β -galactosidase staining and decreased Ki67 and increased H3K9Me2 expression in Western blot analysis. In addition to this senescence there is an increase in apoptosis, and an increased sensitivity to DNA damaging reagents. Thus, over-expression of Sim2s promotes a decrease in cellular growth, and decreased viability when treated with genotoxic reagents (Figure 21).

Because the work presented here will be used as a foundation for future studies, several issues need to be addressed. First, confirmation of up- or down-regulation of Sim2s by Western blot needs to be optimized. While Real Time PCR shows an up-regulation of the RNA (with over-expression), it is the stabilization of the protein that needs to be observed. Secondly, cells over-expressing Sim2s are also seen to arrest in S-phase. Unfortunately we were unable to investigate this unique finding here, but future work will be done in this direction. Thirdly, an alternative control (un-transduced MCF7 cells) could have been used to fully verify these findings. Finally, several of the assays presented here need to be repeated—especially Western blot analysis of H3K9Me2, as the findings are intriguing (with no observable expression in control cells and extreme up-regulation in Sim2s cells). These results need to be further verified.

Additionally, future work will delineate the mechanism by which Sim2s is activated by DNA damage and how this activation results in up-regulation of p21. The role Sim2s plays in interacting with both p53 and p21 will be further clarified. While we observed that p21 was induced in a p53-independent fashion, p53 was induced in MCF7 cells in which Sim2s has been knocked-down across the board, while p53 was only active in Sim2s over-expressing cells in response to DNA damage. The possible interaction with p53 is an extremely important aspect to examine. Future work will also involve observing whether Sim2s is capable of directly interacting with p21 via CHIP and CoIP analysis. Ultimately, understanding the mechanistic role Sim2s plays in response to DNA damage and cell cycle arrest will help us better understand its role as a potential tumor suppressor in the mammary gland.

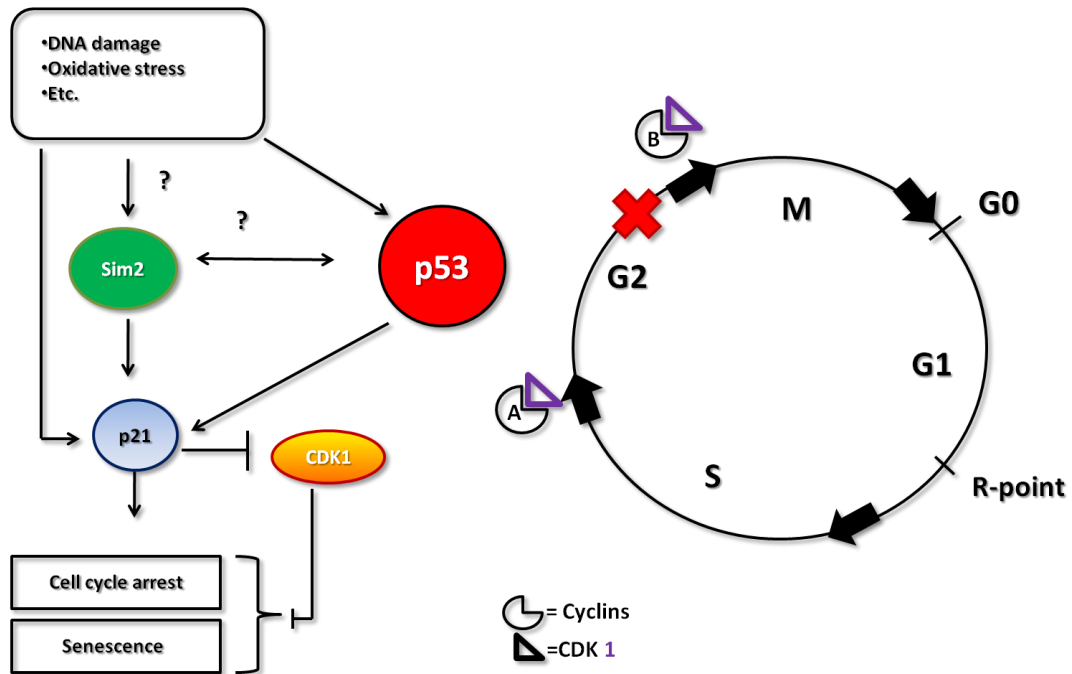


Figure 21. Proposed role of Sim2s in cell cycle arrest and cellular senescence. DNA damage results in induction of p21—perhaps by the transcription factor Sim2s. Over-expression of Sim2s results in up-regulation of p21—which results in cell cycle arrest and cellular senescence. In addition to this observed senescence, cells over-expressing Sim2s are sensitized to DNA damaging reagents, possibly through a similar mechanism that results in cellular senescence.

REFERENCES

1. American Cancer Society. Cancer Facts and Figures [Report]. Atlanta: American Cancer Society; 2009.
2. McIntosh BE, Hogenesch JB, Bradfield CA. Mammalian Per-Arnt-Sim proteins in environmental adaptation. *Annu Rev Physiol.* 2010;72:625-45.
3. Chang J, Kim IO, Ahn JS, Kim SH. The CNS midline cells control the spitz class and Egfr signaling genes to establish the proper cell fate of the Drosophila ventral neuroectoderm. *Int J Dev Biol.* 2001;45:715-24.
4. Nambu JR, Lewis JO, Wharton KA, Jr., Crews ST. The Drosophila single-minded gene encodes a helix-loop-helix protein that acts as a master regulator of CNS midline development. *Cell.* 1991;67:1157-67.
5. Coumailleau P, Duprez D. Sim1 and Sim2 expression during chick and mouse limb development. *Int J Dev Biol.* 2009;53:149-57.
6. Michaud JL, Rosenquist T, May NR, Fan CM. Development of neuroendocrine lineages requires the bHLH-PAS transcription factor SIM1. *Genes Dev.* 1998;12:3264-75.
7. Goshu E, Jin H, Fasnacht R, Sepenski M, Michaud JL, Fan CM. Sim2 mutants have developmental defects not overlapping with those of Sim1 mutants. *Mol Cell Biol.* 2002;22:4147-57.
8. Metz RP, Kwak HI, Gustafson T, Laffin B, Porter WW. Differential transcriptional regulation by mouse single-minded 2s. *J Biol Chem.* 2006;281:10839-48.

9. Wellberg E. Regulation of mammary lactogenic differentiation by single-minded-2s [Dissertation]. Texas A&M University, College Station; 2009.
10. Wellberg E, Metz RP, Parker C, Porter WW. The bHLH/PAS transcription factor single-minded 2s promotes mammary gland lactogenic differentiation. *Development*. 2010;137:945-52.
11. Chrast R, Scott HS, Madani R, Huber L, Wolfer DP, Prinz M, et al. Mice trisomic for a bacterial artificial chromosome with the single-minded 2 gene (Sim2) show phenotypes similar to some of those present in the partial trisomy 16 mouse models of Down syndrome. *Hum Mol Genet*. 2000;9:1853-64.
12. Ema M, Ikegami S, Hosoya T, Mimura J, Ohtani H, Nakao K, et al. Mild impairment of learning and memory in mice overexpressing the mSim2 gene located on chromosome 16: an animal model of Down's syndrome. *Hum Mol Genet*. 1999;8:1409-15.
13. Hasle H. Pattern of malignant disorders in individuals with Down's syndrome. *Lancet Oncol*. 2001;2:429-36.
14. Yang Q, Rasmussen SA, Friedman JM. Mortality associated with Down's syndrome in the USA from 1983 to 1997: a population-based study. *Lancet*. 2002;359:1019-25.
15. Hasle H, Clemmensen IH, Mikkelsen M. Risks of leukaemia and solid tumours in individuals with Down's syndrome. *Lancet*. 2000;355:165-9.

16. Farrall AL, Whitelaw ML. The HIF1 α -inducible pro-cell death gene BNIP3 is a novel target of SIM2s repression through cross-talk on the hypoxia response element. *Oncogene*. 2009;28:3671-80.
17. Kwak HI, Gustafson T, Metz RP, Laffin B, Schedin P, Porter WW. Inhibition of breast cancer growth and invasion by single-minded 2s. *Carcinogenesis*. 2007;28:259-66.
18. Laffin B, Wellberg E, Kwak HI, Burghardt RC, Metz RP, Gustafson T, et al. Loss of single-minded-2s in the mouse mammary gland induces an epithelial-mesenchymal transition associated with up-regulation of slug and matrix metalloproteinase 2. *Mol Cell Biol*. 2008;28:1936-46.
19. Massague J. G1 cell-cycle control and cancer. *Nature*. 2004;432:298-306.
20. Lindqvist A, Rodriguez-Bravo V, Medema RH. The decision to enter mitosis: feedback and redundancy in the mitotic entry network. *J Cell Biol*. 2009;185:193-202.
21. Matsuoka S, Rotman G, Ogawa A, Shiloh Y, Tamai K, Elledge SJ. Ataxia telangiectasia-mutated phosphorylates Chk2 in vivo and in vitro. *Proc Natl Acad Sci U S A*. 2000;97:10389-94.
22. Bartek J, Lukas J. Mammalian G1- and S-phase checkpoints in response to DNA damage. *Curr Opin Cell Biol*. 2001;13:738-47.
23. Beckerman R, Donner AJ, Mattia M, Peart MJ, Manley JL, Espinosa JM, et al. A role for Chk1 in blocking transcriptional elongation of p21 RNA during the S-phase checkpoint. *Genes Dev*. 2009;23:1364-77.

24. Falck J, Mailand N, Syljuasen RG, Bartek J, Lukas J. The ATM-Chk2-Cdc25A checkpoint pathway guards against radioresistant DNA synthesis. *Nature*. 2001;410:842-7.
25. Taylor WR, Stark GR. Regulation of the G2/M transition by p53. *Oncogene*. 2001;20:1803-15.
26. Evan GI, d'Adda di Fagagna F. Cellular senescence: hot or what? *Curr Opin Genet Dev*. 2009;19:25-31.
27. Prieur A, Peeper DS. Cellular senescence in vivo: a barrier to tumorigenesis. *Curr Opin Cell Biol*. 2008;20:150-5.
28. Adams PD. Healing and hurting: molecular mechanisms, functions, and pathologies of cellular senescence. *Mol Cell*. 2009;36:2-14.
29. el-Deiry WS, Tokino T, Waldman T, Oliner JD, Velculescu VE, Burrell M, et al. Topological control of p21WAF1/CIP1 expression in normal and neoplastic tissues. *Cancer Res*. 1995;55:2910-9.
30. Sarkisian CJ, Keister BA, Stairs DB, Boxer RB, Moody SE, Chodosh LA. Dose-dependent oncogene-induced senescence in vivo and its evasion during mammary tumorigenesis. *Nat Cell Biol*. 2007;9:493-505.
31. Bartkova J, Rezaei N, Liontos M, Karakaidos P, Kletsas D, Issaeva N, et al. Oncogene-induced senescence is part of the tumorigenesis barrier imposed by DNA damage checkpoints. *Nature*. 2006;444:633-7.
32. Mallette FA, Ferbeyre G. The DNA damage signaling pathway connects oncogenic stress to cellular senescence. *Cell Cycle*. 2007;6:1831-6.

33. Serrano M, Lin AW, McCurrach ME, Beach D, Lowe SW. Oncogenic ras provokes premature cell senescence associated with accumulation of p53 and p16INK4a. *Cell*. 1997;88:593-602.
34. Vafa O, Wade M, Kern S, Beeche M, Pandita TK, Hampton GM, et al. c-Myc can induce DNA damage, increase reactive oxygen species, and mitigate p53 function: a mechanism for oncogene-induced genetic instability. *Mol Cell*. 2002;9:1031-44.
35. Ohtani N, Mann DJ, Hara E. Cellular senescence: its role in tumor suppression and aging. *Cancer Sci*. 2009;100:792-7.
36. Lee J, Kim JA, Barbier V, Fotedar A, Fotedar R. DNA damage triggers p21WAF1-dependent Emil down-regulation that maintains G2 arrest. *Mol Biol Cell*. 2009;20:1891-902.
37. Chang BD, Broude EV, Fang J, Kalinichenko TV, Abdryashitov R, Poole JC, et al. p21Waf1/Cip1/Sdi1-induced growth arrest is associated with depletion of mitosis-control proteins and leads to abnormal mitosis and endoreduplication in recovering cells. *Oncogene*. 2000;19:2165-70.
38. Menne TV, Luer K, Technau GM, Klambt C. CNS midline cells in *Drosophila* induce the differentiation of lateral neural cells. *Development*. 1997;124:4949-58.
39. Vermeulen K, Van Bockstaele DR, Berneman ZN. The cell cycle: a review of regulation, deregulation and therapeutic targets in cancer. *Cell Prolif*. 2003;36:131-49.

40. Macleod KF, Sherry N, Hannon G, Beach D, Tokino T, Kinzler K, et al. p53-dependent and independent expression of p21 during cell growth, differentiation, and DNA damage. *Genes Dev.* 1995;9:935-44.
41. Cairney CJ, Sanguinetti G, Ranghini E, Chantry AD, Nostro MC, Bhattacharyya A, et al. A systems biology approach to Down syndrome: identification of Notch/Wnt dysregulation in a model of stem cells aging. *Biochim Biophys Acta.* 2009;1792:353-63.
42. Coppede F, Migliore L. DNA repair in premature aging disorders and neurodegeneration. *Curr Aging Sci.* 2010;3:3-19.
43. Collado M, Serrano M. Senescence in tumours: evidence from mice and humans. *Nat Rev Cancer.* 10:51-7.

VITA

Name: Lauren M. Schilling

Address: Texas A&M University
Genetics Department
2128 TAMU
College Station, TX 77843-2128

Email Address: LSchilling@cvm.tamu.edu

Education: B.S., Biomedical Sciences, Texas A&M University, 2006
M.S., Genetics, Texas A&M University, 2010